Russian Chemical Reviews **69** (10) 821 – 843 (2000) © 2000 Russian Academy of Sciences and Turpion Ltd

DOI 10.1070/RC2000v069n10ABEH000605

Quantum-size colloid metal systems

V I Roldughin

Contents

I.	Introduction	821
II.	Methods for the synthesis of metal nanoparticles	822
III.	Methods for calculation of the electronic properties of metal nanoparticles	825
IV.	The electronic and thermodynamic properties of small metal particles and thin films	829
V.	Optical properties of small particles	832
VI.	The influence of radiation on the stability of nanoparticles	834
VII.	Relaxation of electrons in small particles	835
VIII.	Electron transfer through nanoparticles	836
IX.	Self-assembly of nanoparticles	837
X.	Conclusion	839

Abstract. Methods for the preparation of nano-sized metal particles are considered. Theoretical approaches to the analysis of electron behaviour in systems with quantum-size effects are outlined. The results of experimental investigations of the thermodynamic and optical characteristics of small metal particles and thin films are presented. The data of experiments on the electron dynamics in single nanoparticles and nanoparticle ensembles are described. The self-assembly of nanoparticles to form supported ordered structures is considered. The bibliography includes 343 references.

I. Introduction

The interest of researchers in nano-sized systems has markedly enhanced in recent years. Two main lines have taken shape in the research and practical application of systems consisting of elements with sizes from several nanometers to hundred nanometers. The first line includes studies of nano-structured materials. These materials are formed by a large number of nano-sized particles the individual properties of which show themselves in an indirect way — the change in the properties of individual structural units on passing to the nanometer region results in the appearance of new properties of the material. Thus, the ceramics produced from nanometer particles possess enhanced strength, plasticity and wear resistance; alloys of non-compatible metals can be formed; the electrical and magnetic properties of the composites are enhanced, and so on. The achievements concerning imparting new properties to nano-structured materials have been described in the literature fairly comprehensively.[1,2] Therefore, we do not consider these aspects here.

The second line of research is related to studies of individual nanoparticles. The goals of these studies include both the development of methods for the preparation of nanoparticles which would allow one to manipulate them as separate objects and investigation into the physicochemical properties of the nanoparticles synthesised. The history of development of these investigations is fairly long; the results are reflected in monographs.[3,4]

However, after the publication of these monographs, many new results not reflected yet in review literature have been obtained. The greater part of the experimental data concerning the synthesis and study of the properties of nanoparticles appeared during the last decade. This enhancement of the interest in nanoparticles is due to several reasons

— methods for controlling the size of nanoparticles have been developed;

— new methods for the experimental investigation of nanoparticle structures and electronic and optical characteristics have appeared;

— procedures which enable isolation and stabilisation of individual nanoparticles together with the investigation of their physicochemical properties have been elaborated;

— finally, new properties of nanoparticles were discovered which permit them to be regarded as promising elements of microelectronic devices. The progress attained in the synthesis and study of nanoparticles brought about new problems, which have also stimulated new experimental studies.

In this review, we consider only some of the problems related to the 'quantum-size' colloid metal systems. One should bear in mind the difference between nano-sized (or quantum-size) particles and ultradisperse systems. The latter term has long been used in colloid chemistry. It refers to systems consisting of particles the size of which is smaller than 100 nm; in this case, the contribution of the surface to the thermodynamic characteristics becomes significant, which implies the possibility of changing the surface properties, for example, the surface tension (size corrections). The bulk properties of the particles are usually considered invariant. Meanwhile, the term nano- or quantum-size particles is used to imply colloidal systems of particles, the bulk characteristics of which undergo changes of one type or another caused by particle dimensions. It is this type of systems that is discussed below.

Attention is focused on the preparation of metal nanoparticles in colloidal solutions and on the thermodynamic properties of nanoparticles and metallic films under conditions where quantisation of the electron movement plays a noticeable role. Simulta-

V I Roldughin Institute of Physical Chemistry, Russian Academy of Sciences, Leninsky prosp. 31, 117915 Moscow, Russian Federation. Fax (7-095) 952 53 08. Tel. (7-095) 955 46 47.
E-mail: roldugin@phyche.ac.ru

Received 22 May 2000
Uspekhi Khimii **69** (10) 899 – 923 (2000); translated by Z P Bobkova

neously, the main methods used to calculate the electronic structures and thermodynamic characteristics of quantum-size metal systems are outlined. The features of electron dynamics in small metal particles are described and the collective effects in the colloidal ensembles of nanoparticles are considered.

We wittingly restricted consideration to colloidal systems based on metal particles because other nano-sized systems as well as methods for their synthesis and study of properties have already been described in review literature. For example, the results of investigations into the synthesis and encapsulation of nanoparticles in various organic matrices have been reported [5, 6] and various aspects of the physical chemistry of semiconductor nanoparticles have been analysed comprehensively in a review.[7] In addition, the experimental data concerning nano-sized systems are so numerous that it is impossible to embrace the whole body of information available from the literature in one review.

II. Methods for the synthesis of metal nanoparticles

There exist diverse methods for the preparation of nanoparticles and nanocomposites. In this Section, we shall consider several main methods used to prepare nanoparticles which ensure the possibility of isolating them and separating them from the ensemble. Nanoparticles can present interest as elements of microelectronic devices only when they have been isolated from the ensemble. Therefore, the problem of preparing individual nanoparticles is one of the central problems in today's investigations.

1. Evaporation – condensation method

The evaporation – condensation method has long served as a common method for the preparation of metal nanoparticles.[3] According to this method, a metal is evaporated into a flow of an inert gas. Then the flow of the carrier gas with the metal vapour is fed to a chamber, while the temperature of the chamber walls varies according to a previously specified pattern. The pattern of temperature variation is usually calculated taking into account the heat and mass transfer equations and the kinetics of nucleation, in order to attain the necessary rate of condensation of the metal vapour such that the particles have time to grow to the required size before supersaturation is eliminated.

Until recently, the particles thus prepared have been deposited on an inert substrate.[3, 8] The use of a support was necessary in the gas-phase method. Only in this case, were individual particles produced because nano-sized particles are fairly mobile and stick together upon collision; hence, their aggregation has to be suppressed somehow.

Detailed investigations [9] into the kinetics of aggregation of nanoparticles during their preparation by the evaporation – condensation method have shown that, for example, zinc nanometer particles aggregate over periods of 10 – 100 ms depending on the conditions of particle growth. They form fractal aggregates with log-normal size distribution, the average size of the aggregates corresponding to the micrometer range.

The evaporation – condensation procedure gives rise to the purest metal particles. This is why it still remains attractive; however, search for the methods that would enable the preparation of nanoparticles without using solid supports is in progress. Methods have been proposed [10 – 14] in which the solid support was replaced by frozen argon [10] or by a solvent.[11, 14] According to these (and other similar) techniques, the particles are co-precipitated with the solvent; thus, a composite containing nanoparticles gradually grows. By subsequent heating, the solid composite is converted into a colloidal dispersion of nanoparticles.

Colloidal dispersions obtained in this way are not always stable. In order to obtain stable systems, the methods mentioned above have been modified,[15, 16] namely, surfactants were introduced into the system by co-precipitation (or added subsequently). This gave particles with sizes of up to 1 nm dispersed in a solvent with a concentration of 10^{20} particles per m^3. According to the data of electron microscopy, systems prepared in this way contained no particle aggregates.

In early studies,[15, 16] evaporation – condensation experiments were performed with silver particles. This method was studied in more detail in another study in which Ag, Bi, Cu and Te nanoparticles were obtained.[17] It was found that particles with the size from 1 to 10 nm can be obtained in any of the systems tested by varying the pressure and the composition of the carrier gas. The particle size varies as a linear function of pressure. The particles are characterised by a rather narrow size distribution, the corresponding standard deviation being 1.4 – 1.6.

Particles of Ag/M alloys (M = Co, Fe, Ni) with approximately the same characteristics were also prepared by the evaporation – condensation technique.[18]

An aerosol method for the preparation of silver nanoparticles coated with a dodecanethiol layer and subsequent introduction of the particles into an organic solvent have been reported.[19, 20] Coating with dodecanethiol was accomplished in the vapour phase immediately after the nucleation of particles by mixing of an aerosol flow with a flow of an inert gas saturated by dodecanethiol vapour. This procedure provided nanoparticles with the best dispersity; however, this was associated with substantial procedural difficulties.

Despite the progress achieved using the evaporation – condensation method, it is mainly employed to produce composite materials and is seldom used to prepare nanoparticles. This is due, first, to the low productivity of the method and, second, to the fact that the size distribution of the resulting particles is too broad, according to the modern criteria. In addition, when using this method, it is difficult to control the size of the nanoparticles formed. As a consequence, standard colloidal methods for the preparation of nanoparticles proved to be more convenient; they have become more attractive owing to the unexpectedly successful use of special surfactants.

2. Reduction from solutions

Chemical reduction is used most widely to synthesise colloidal particles.[21] Metal salts can be reduced by various reducing agents in the presence of stabilisers (special ligands, polymers, surfactants), which suppress particle aggregation.[22, 23] The reduction yields particles of different sizes. The size cannot be predicted because it is affected simultaneously by several factors: the nature and the concentration of the solvent and the stabilising agent used, reaction temperature, and reaction time. In addition, the particle size is determined to a large extent by the supersaturation developed, higher supersaturation resulting in smaller particles; hence, the size of the particles can be controlled by varying supersatruration.[21, 24]

The degree of supersaturation reached in the experiments is governed by the rate of the chemical reduction, temperature and the amount of the reduced metal spent for the particle formation and growth. The process of particle formation is normally connected with homogeneous (or, perhaps, heterogeneous) nucleation. As a rule, it is limited by the experimental conditions. For this reason, the main way of controlling the particle size is to use growth retardants, which play a dual role. On the one hand, they retard the transfer of the reduced metal from the solution to the particles and thus increase supersaturation. On the other hand, the retardants directly limit the rate of the increase in the particle size. Thus, the choice of the protective shell of the particles appears to be the crucial point in controlling the particle size.

Alkanethiols are known to form dense self-assembled monolayers on the surface of crystalline gold.[25] However, until recently, this fact has not been used in the synthesis of nanoparticles. Only in a few publications,[26, 27] were alkanethiols employed in the reduction of gold in a solution of $HAuCl_4$ by $NaBH_4$; it was found that this process yields virtually monodisperse particles. Originally, so-called two-phase method consisting of two stages has been used for reduction.[26, 27] In the first stage, metal-contain-

ing reagents were transferred from the aqueous phase to the organic phase and then solutions of the surfactant and the reducing agent were added to the organic phase. Subsequently, a single-phase method was developed.[28–34] According to this method, solutions of the surfactant and the reducing agent were added simultaneously to a metal-containing solution. Presumably, in both cases, gold is reduced to the atomic state, which ends in the nucleation of atoms to give nanocrystals; alkanethiols are adsorbed on the surface of the crystals. The thermodynamics of formation of gold nanoparticles in the presence of alkanethiols has been considered in a study,[30] where it was shown that the process of formation of nanoparticles is similar to the process of formation of drops of a water-in-oil microemulsion.

The gold nanocrystals coated by an alkanethiol monolayer, which are formed upon reduction, consist of a metallic core comprising 10 to 5000 atoms and a dense surfactant shell. Almost all the particles exhibit a clear-cut plasmon band in the optical absorption spectrum. The position and the width of the band depend on the particle size and the properties of the adsorbed layer.

The monolayer on nanoparticles is assumed to be self-assembled in the same way as on the surface of bulk samples. The size of nanocrystals depends on the length of the alkyl chain in alkanethiol and on the thiol to gold ratio in the solution.[27, 32, 35] Examination by electron microscopy shows that gold microcrystals are compact and faceted and have a face-centred cubic (FCC) lattice.[32] The crystals are mainly octahedral or icosahedral. The inner area of the microcrystals is pure gold, the sulfur atoms being located on the surface and connected to alkyl chains. These results were obtained from spectroscopy and mass spectrometry.[32, 36, 37]

Arnold and Reilly [37] reported a unique experiment. After the powder of gold nanoparticles coated by alkanethiols had been prepared, it was exposed to powerful laser radiation. As a result, the particles were 'evaporated'. The flow of particles was again irradiated by a laser with the wavelength selected in such a way as to cleave the bond between sulfur and the alkyl chain. This yielded gold nanoparticles with an adsorbed layer of sulfur atoms. The resulting clusters were studied by mass spectrometry. Interpretation of the mass spectra showed that the sulfur atoms form dense monolayers on the surface of gold microcrystals. This result fully confirmed the assumption concerning the formation of dense self-assembled monolayers of alkanethiols on the surface of gold nanoparticles.

A study has been devoted to the dependence of the structure of alkanethiol adlayers coating nanoparticles on the particle size.[38] Particles with sizes ranging from 1.2 to 5.2 nm were used in these experiments. The properties of the adlayer were studied by Fourier transform IR spectroscopy, differential scanning calorimetry, wetting and thermal desorption mass spectrometry. The transition from a two-dimensional to three-dimensional packing of alkanethiol molecules was also investigated. It was found that in the case of larger nanoparticles, more ordered conformations of the alkyl chains in the adsorbed alkanethiols are observed. The critical diameter corresponding to the change in the pattern of the adlayer packing was found to be 4.4 nm. For particles with larger diameters, a two-dimensional adlayer is formed, whereas in the case of particles with smaller diameters, elements of a three-dimensional packing show themselves in the adlayer.

In recent years, more complex thiolates have been used for the production of gold nanoparticles,[39–43] because surfactants with more complicated structures may promote the formation of self-assembled monolayers of nanoparticles (see below). The method is being perfected;[44] this allows preparation of particles of different metals according to the same procedure.

In particular, alkanethiols have been employed to produce silver nanoparticles [45–50] (by both single-phase and two-phase procedures). Simultaneous synthesis of gold, silver and platinum nanoparticles has also been accomplished.[51] As for gold, in this case, too, the position of the plasmon band in the optical absorption spectra depended on the method of preparation and the structure of the environment of metal particles.

3. Reduction in microemulsions

Microemulsions of the 'water-in-oil' type (reverse micelles) have been attracting increasing attention in recent years as microreaction media for the preparation of nanoparticles. Microemulsions consist of nano-sized water (or solution) drops dispersed in oil (organic) phase and stabilised by surfactant molecules distributed over the interface. Highly dispersed drops of water are perfect microreactors for the preparation of nanoparticles because the size of drops is a natural restrictor for the dimensions of the growing nanoparticles.

Primarily, microemulsions have been used for the preparation of monodisperse microparticles. The synthesis of Pt, Pd, Rh and Ir particles by the reduction of the corresponding salts in water drops has been described.[52] Since this publication appeared, microemulsions have been repeatedly used for the preparation of diverse particles of both individual metals and their compounds.

In the 90s, the use of microemulsions to prepare silver,[53–55] gold,[53] platinum, cobalt [56] and iron [57] nanoparticles was reported. Nanoparticles were prepared by reduction of the corresponding metal salts by sodium tetrahydroborate or hydrazine. The unique opportunities for controlling the size and shape of nanoparticles from microemulsions have been demonstrated in several studies.[58–61] The high efficiency of microemulsions in preparing nanoparticles of specified dimensions and shapes was demonstrated most vividly in several studies by Pileni *et al.* [62–67]. In these works, a functional surfactant, copper bis(2-ethylhexyl)sulfosuccinate $Cu(AOT)_2$, was used to prepare copper nanoparticles. The surfactant played a dual role — on the one hand, it stabilised drops of water and, on the other hand, it served as a source of copper in the drops.

To prepare nanoparticles, a microemulsion of water drops stabilised by $Cu(AOT)_2$ and Na(AOT) in isooctane was mixed with a microemulsion of drops of a solution of sodium tetrahydroborate stabilised by Na(AOT). After microemulsions have been mixed, the material exchange between the drops starts and copper is reduced. Due to the presence of natural restrictions, the resulting copper particles are nano-sized.

The size and shape of particles are largely determined by the ratio

$$w = \frac{[H_2O]}{[AOT]}$$

in the microemulsion, because the structure of the microemulsion also depends significantly on this ratio. When $w < 4$, only spherical drops are present, their size being proportional to w. Reduction of copper in such a system gives rise to spherical nanoparticles 1 to 12 nm in diameter; their size is also proportional to w.

Further increase in the content of water ($4 < w < 5.5$) changes the shape of microdrops — they become spheroidal. Correspondingly, reduction in the system affords spherical nanoparticles with diameters of 8.2 and 12 nm and cylindrical particles with a diameter of 12 nm and a length of 18.5 nm. When the relative water content is $5.5 < w < 11$, the microemulsion has a structure of a bi-continuous phase in which nano-spheres with diameters of 6.7 and 9.5 nm and 22.6-nm long nano-rods 9.5 nm in diameter are formed.

When the content of water increases further ($w > 11$), the microemulsion is transformed into a lamellar structure in which only rods with lengths of 300 to 1500 nm and with diameters of 10 to 30 nm are present. According to electron microscopy data, nanoparticles synthesised in microemulsions (including the long rods mentioned above) have defect-free surfaces, which indicates their high quality.

The process of reduction of nanoparticles in microemulsions was studied by numerical modelling by the Monte Carlo method.[68–70] The modelling data showed that the flexibility of

the surfactant monolayer and the surfactant concentration in the system play an important role in the formation of particles in microemulsions. By varying the monolayer flexibility and the content of the surfactant, one can change appreciably the size distribution of nanoparticles and even prepare ensembles with a bimodal size distribution, which is apparently due to the character of evolution of the supersaturation of microemulsions with metal atoms.[24]

Since surfactants play an important role in the preparation of nanoparticles in microemulsions, the search for new, in particular, non-ionic surfactants which could be used in the synthesis of metal nanoparticles is currently in progress.[71] Syntheses are carried out using non-traditional microemulsions such as water drops in supercritical carbon dioxide.[72]

In view of the significant dependence of the size distribution of particles on the character of the exchange of matter between the drops, the use of new methods for the synthesis of nanoparticles in microemulsions which exclude this exchange has started. For example, Revina *et al.*[73,74] prepared silver nanoparticles by radiation-induced reduction. Studies on the influence of external factors, for example, temperature,[75,76] on the size and shape of nanoparticles formed in microemulsions have been carried out (in the studies cited, these were gold nanoparticles).

4. Preparation of nanoparticles with a stoichiometric composition

A method yielding metal nanoparticles with a definite composition is most promising as regards investigation of the individual properties of these particles. Primarily, these particles were obtained as metal clusters containing less than ten and, later, more than ten metal atoms (a brief review of the history of preparation of these compounds has been reported[77]). Substantial progress along this line has been achieved by Vargaftik *et al.*,[78–80] who identified unambiguously palladium clusters containing (in the ideal case) exactly 561 metal atoms. The cluster had the composition $Pd_{561}L_{60}(OAc)_{180}$, where L is 1,10-phenanthroline or 2,2′-bipyridine and the OAc groups form the ligand shell. The cluster was produced in a two-stage synthesis[78–80] including the reduction of $Pd(OAc)_2$ with hydrogen in an AcOH solution

$$Pd(OAc)_2 + L + H_2 \longrightarrow (1/n)[Pd_4H_4(OAc)L]_n + AcOH$$

and subsequent treatment of the high-molecular-weight clusters with oxygen

$$[Pd_4H_4(OAc)L]_n + O_2 + AcOH \longrightarrow$$
$$\longrightarrow Pd_{561}L_{60}(OAc)_{180} + Pd(OAc)_2 + L + H_2O.$$

This cluster belongs to the category of 'magic clusters',† *i.e.* those containing strictly definite, 'magic' numbers of metal atoms, namely, 13, 55, 147, 309, 561, ... These numbers correspond to fully occupied atomic layers (shells) of cubooctahedral clusters having a FCC lattice. No clusters with three filled shells have been synthesised up to now;[81] however, clusters with four[82] ($Pt_{309}Phen_5O_{30}$, Phen is *o*-phenanthroline) and five[78,83] ($Pd_{561}Phen_{36}O_{200}$) shells have been prepared. The existence of clusters with seven[84] ($Pd_{1415}Phen_{54}O_{1000}$) and eight[85] ($Pd_{2057}Phen_{38}O_{1600}$) shells has also been established. The clusters obtained were studied by various methods — high-resolution electron microscopy, EXAFS, Mössbauer spectroscopy, NMR and others. These studies demonstrated that metal atoms actually form a close cubic packing and the distance between the metal atoms virtually coincides with that found for bulk samples. The diameter of the metallic core of the clusters varies from 2.4 to 3.7 nm.

† The matter concerns 'magic' numbers in terms of the Mackay–Chini crystal-chemical model. See A L Mackay *Acta Cystallogr.* **15** 225 (1979); P Chini *J. Organomet. Chem.* **200** 37 (1980); B K Teo, N J A Sloan *Inorg. Chem.* **24** 4545 (1985).

The mechanism which provides the synthesis of clusters with a definite number of metal atoms according to the above-described scheme has not been ultimately elucidated. Investigations into the structures of the cluster precursors at different stages of evolution showed that they are shaped like polymeric chains, which are transformed into compact metal particles during heat treatment.[86] In the case of the cluster with the Pd_{561} core, the metal particle forms a FCC lattice and takes on an icosahedral or twin shape at the final stage.[87–89]

The methods for the preparation and investigation of clusters with a specified number of atoms are being constantly improved. Modern methods have been employed to perform unique investigations of the thermodynamic and magnetic properties of these nanoparticles. It will be shown below that physical characteristics of 'quantum'-size particles depend essentially on the number of collective electrons they contain.

5. Other methods for the preparation of metal nanoparticles

Among other methods used to synthesise metal nanoparticles, apart from those described above, mention should be made of pulse radiolysis in solutions, which is employed fairly frequently.[90–97] Under the action of X-ray or ultraviolet radiation or of high-energy electrons, clusters M_2^+, M_3^+, ... , M_n^{x+} are formed successively.[98] Some of these are exceptionally stable. As a result, stable magic clusters are accumulated in the solution. The presence of magic clusters is indicated by the appearance of characteristic bands in the absorption spectra. The contribution of 'non-magic' clusters was found to be insignificant because their lifetimes are fairly short. When using the radiolysis method to prepare nanoparticles, various stabilisers are also added, although in some cases, for example, for aqueous solutions of silver, the use of stabilisers is optional. The nanoparticles formed in the presence of stabilisers are characterised by a higher level of monodispersity and a smaller size. Polymers are used as stabilisers.[99] The method of radiolysis is also applicable for the preparation of nanoparticles with a mixed composition.[100,101] This is done either by the reduction of different metal ions present simultaneously in the solution or by preparing first the particles of one metal and coating them subsequently with a shell of a different metal,[102] which is also reduced by radiolysis. By varying radiation doses, one can control the size and the composition of nanoparticles. Apart from the radiation-chemical method, sonochemical preparation of particles is also used.[103]

Metal nanoparticles are often prepared in the presence of polymers.[104–120] Soluble polymers,[104–109,118–120] block copolymers[115,116] or cross-linked matrices are used. The role of the polymeric medium is usually to stabilise the particles. In addition, in the case of solutions of polymers or block copolymers subjected to microphase separation,[116] they restrict the particle size. The extent to which the polymer influences the size of nanoparticles depends on the length of the polymer chain[119] and on the conditions of synthesis. The synthesis can require a fairly sophisticated procedure; for example, nanoparticles have been prepared using supercritical carbon dioxide.[111] In another study,[120] polymers were used to ensure high yields of nanoparticles of noble metals. One more problem was solved simultaneously, namely, transfer of the nanoparticles into a colloidal solution of any concentration, replacement of the solvent being possible.

Various templates are used in the synthesis of nanoparticles in order to impart a specified shape to them and to restrict their size. The materials used for this purpose included polymeric membranes[121,122] (this permitted the researchers to grow cylindrical particles), high-porosity oxide films[123] and specially prepared substrates,[124–126] which often provided the possibility of preparing catalysts ready for use or ordered structures constructed from nanoparticles. In some cases, nanoparticles and composites based on them are prepared using the 'sol–gel' technology,[127–132] or by growing particles in biological[133,134] and liquid-crystalline[135] systems. A method for the preparation of nanoparticles under electric discharge in solution has been proposed.[136]

III. Methods for calculation of the electronic properties of metal nanoparticles

1. The density functional method

The *ab initio* Hartree–Fock method has found wide use in the calculation of properties of many-electron systems. In this method, the properties of a many-particle system are determined by calculating the orbitals of separate electrons moving in the self-consistent field of other electrons and atomic nuclei. The Hartree–Fock method allows one to find the wave functions of electrons without invoking adjustable parameters. The main obstacle to the use of this method is the complexity of calculations; the time it takes to perform calculations increases as N^4, where N is the number of electrons in the system. For this reason, the Hartree–Fock method is mainly used to perform calculations for atoms or relatively small molecules and clusters.

The greatest progress in calculations for many-electron systems has been attained in the last decades using the density functional method. The time needed for calculations by this method increases with an increase in the number of electrons much more slowly; at present, this method is widely used for calculations for various systems with a large number of electrons including polyatomic molecules, complexes, clusters, and condensed media.

There are two approaches in the density functional method, namely, integral and local approaches. The former dates from an original study by Hohenberg and Kohn,[137] while the latter is a modification of the theory proposed by Kohn and Sham.[138] We shall consider these approaches in relation to a system of N non-relativistic electrons described by a Hamiltonian

$$H = T + V + U. \tag{1}$$

Here T is the operator for the kinetic energy of electrons

$$T = -\frac{1}{2m}\hbar^2 \sum_i \Delta_i\,, \tag{2}$$

m is the mass of an electron, Δ_i is the Laplacian for an ith particle, V is the potential energy operator for a system of electrons in an external field and U is the operator of the electrostatic repulsion energy of electrons.

It was shown [137] that the electron density distribution $\rho(\mathbf{r})$ determines unambiguously all the main properties of a many-electron system including the wave function. The energy of a many-electron system in an external field $v(\mathbf{r})$ is a functional of $\rho(\mathbf{r})$

$$E[\rho(\mathbf{r})] \equiv \int v(\mathbf{r})\rho(\mathbf{r})\mathrm{d}\mathbf{r} + G[\rho(\mathbf{r})]. \tag{3}$$

The last term depends on the wave function Ψ of the system of electrons, determined by the distribution of their density

$$G[\rho(\mathbf{r})] = \int \Psi^*[\rho(\mathbf{r})](T + U)\Psi[\rho(\mathbf{r})]\mathrm{d}\mathbf{r} \tag{4}$$

(the character * means the complex conjugate).

The minimum energy corresponds to the ground state of the system

$$E[\rho(\mathbf{r})] \geqslant E[\rho_g(\mathbf{r})], \tag{5}$$

where $\rho_g(\mathbf{r})$ is the electron density distribution in the ground state.

However, the fundamentality and simplicity of the Hohenberg and Kohn theorem [137] are fraught with latent difficulties. Determination of the electronic density and other characteristics of an electron system requires that the explicit form of functional (3) be known. However, the explicit form of this functional is unknown; thus, additional statements are needed to find the form of $E[\rho(\mathbf{r})]$. Functional (3) can formally be represented as follows:

$$E[\rho(\mathbf{r})] = \int v(\mathbf{r})\rho(\mathbf{r})\mathrm{d}\mathbf{r} + T_0[\rho(\mathbf{r})] + \tag{6}$$

$$+ \frac{1}{2}\int \frac{\mathrm{e}^2\rho(\mathbf{r})\rho(\mathbf{r}')}{|\mathbf{r}-\mathbf{r}'|}\mathrm{d}\mathbf{r}\mathrm{d}\mathbf{r}' + E_{xc}[\rho(\mathbf{r})],$$

where e is the charge of an electron, $\mathbf{r}$, $\mathbf{r}'$ are space coordinates.

The second term is the kinetic energy of non-interacting electrons T_0, and the third term is the energy of electrostatic interaction between them.

The last term, $E_{xc}[\rho(\mathbf{r})]$, is an electron density functional depending implicitly on $v(\mathbf{r})$. It is usually called exchange correlation energy of electron gas. Actually, equality (6) is the definition of this functional. Thus, a fundamental problem faced by the density functional method is to elucidate the form of the functional $E_{xc}[\rho(\mathbf{r})]$. There are several approximate methods for the calculation of this functional.[139]

Minimisation of functional (3) in a one-electron approximation results in a set of self-consistent equations (Kohn–Sham equations)

$$\left(-\frac{1}{2}\frac{\hbar^2}{m}\Delta_j + v(\mathbf{r}) + \int \frac{\mathrm{e}^2\rho(\mathbf{r}')\mathrm{d}\mathbf{r}'}{|\mathbf{r}-\mathbf{r}'|} + v_{xc}(\mathbf{r}) - E_j\right)\varphi_j(\mathbf{r}) = 0. \tag{7}$$

Here, $\rho(\mathbf{r})$ is the electron density

$$\rho(\mathbf{r}) = \sum_{j=1}^{N} \varphi_j^*(\mathbf{r})\varphi_j(\mathbf{r}), \tag{8}$$

$v_{xc}(\mathbf{r})$ is the exchange correlation potential

$$v_{xc}(\mathbf{r}) = \frac{\delta E_{xc}[\rho(\mathbf{r})]}{\delta\rho(\mathbf{r})}\,, \tag{9}$$

E_j are single-electron energy levels, $\varphi_j(\mathbf{r})$ are single-electron wave functions, $j = 1, \ldots, N$.

The ground-state energy for a many-electron system is given in this approximation by the relation

$$E = \sum_{j=1}^{N} E_j - \frac{1}{2}\int \frac{\mathrm{e}^2\rho(\mathbf{r})\rho(\mathbf{r}')}{|\mathbf{r}-\mathbf{r}'|}\mathrm{d}\mathbf{r}\mathrm{d}\mathbf{r}' - \int v_{xc}(\mathbf{r})\rho(\mathbf{r})\mathrm{d}\mathbf{r}\,. \tag{10}$$

Formally, the Kohn–Sham equations are exact; however, there exists the problem of the relationship between $v_{xc}(\mathbf{r})$ and electron density. At present, it can be regarded proven that the potential $v_{xc}(\mathbf{r})$ can be determined unambiguously; in this case, the use of single-electron approximation does not play a crucial role.[140–142] It has also been proven that, by using the potential $v_{xc}(\mathbf{r})$, one can reproduce precisely the distribution of electron density in the system [143] and that the upper occupied level of an isolated system of electrons in the absence of an external field is related uniquely to the ionisation potential;[144] in addition, the asymptotic variation of the electron density for a system with a finite number of electrons is entirely determined by the upper occupied single-electron function (orbital).

As has already been noted, the use of the density functional method requires at least an approximate way of finding $E_{xc}[\rho(\mathbf{r})]$. For a uniform electron gas, it can formally be written in the local density approximation that

$$E_{xc} = \int \rho\varepsilon_{xc}\mathrm{d}\mathbf{r}\,, \tag{11}$$

where ε_{xc} is the local exchange correlation energy of electrons, equal to $-9[(3/4\pi)\rho]^{1/3}$. For non-uniform systems, the local energies ε_{xc} were found as the gradient expansion [145–149]

$$\varepsilon_{xc} = g\left[\rho(\mathbf{r}), \nabla\rho(\mathbf{r}), \nabla^2\rho(\mathbf{r})\right]. \tag{12}$$

Other attempts to determine the exchange correlation energy as the electron density functional have also been undertaken.[150, 151] In particular, it has been represented as a non-local functional.[152]

2. The method of statistical functions

In the investigations of many-electron systems including nanoparticles, considered in this review, the method of statistical distribution functions is also used. This method has been used successfully to study the surface properties of various quantum objects [153–156] and the structures of clusters;[157] it can also be used to investigate the dynamic processes in quantum systems.[156] For this reason, we shall outline briefly the main principles of the distribution functions method.

In quantum mechanics, the role of distribution functions is played by the density matrix [158] for N particles, $\rho N(t)$ (t is time). In the coordinate representation, the density matrix of a system is a function of coordinates and spin variables of all particles

$$\langle\sigma',R'|\rho_N(t)|\sigma,R\rangle = \sum_i P_i\Psi_i^*(R',\sigma')\Psi_i(R,\sigma), \tag{13}$$

where R and σ are sets of coordinates $R = (\mathbf{r}_1, \mathbf{r}_2, \ldots, \mathbf{r}_N)$ and spin variables $\sigma = (\sigma_1, \ldots, \sigma_N)$, and P_i is the probability that the system occurs in a pure state i with the wave function Ψ_i. By means of the density matrix, the average value of any operator $\hat{T}$ can be written in the form

$$\langle\hat{T}\rangle = \sum_\sigma \int \mathrm{d}R\hat{T}\langle\sigma', R'|\rho_N|\sigma, R\rangle\Big|_{\substack{\sigma'=\sigma,\\ R'=R}}, \tag{14}$$

the operator $\hat{T}$ acting on the 'non-primed' variables of the density matrix. After the action of the operator, the primed and non-primed variables are taken to be equal.

The diagonal elements of the density matrix $\langle\sigma, R|\rho_N|\sigma, R\rangle$ determine the probabilities of distribution of the system over coordinates and spin states of the particles.

The density matrix satisfies the Liouville quantum equation

$$\left(i\hbar\frac{\partial}{\partial t} - \hat{H} + \hat{H}'^*\right)\langle\sigma', R'|\rho_N|\sigma, R\rangle = 0. \tag{15}$$

Here $\hat{H}$ is the Hamiltonian for a system of particles acting on the non-primed variables, while $\hat{H}'$ acts on primed variables.

For a system of particles with pair interaction, in the absence of an external field, the Hamiltonian has the form

$$\hat{H} = \sum_i\left(-\frac{\hbar^2}{2m}\Delta_i\right) + \sum_{1\leqslant i<j\leqslant N} u(\mathbf{r}_i - \mathbf{r}_j),$$

where Δ_i is the Laplacian operating on the coordinates of an ith particle and $u(\mathbf{r}_i - \mathbf{r}_j)$ is the energy of pair interaction of particles.

Wigner [159] introduced a special (mixed) representation for a density matrix in which the distributions of particles over coordinates $R = (\mathbf{r}_1, \ldots, \mathbf{r}_N)$ and momenta $P = (\mathbf{p}_1, \ldots, \mathbf{p}_N)$ appear. The density matrices in the Wigner representation and those in the coordinate representation are related as

$$F(R,P,t) = \frac{1}{(2\pi)^{3N}}\int \mathrm{d}\tau[\exp(-i\tau P)] \times \times \langle\sigma, R - \frac{\hbar}{2}\tau|\rho_N(t)|\sigma, R + \frac{\hbar}{2}\tau\rangle, \tag{16}$$

where $\tau = (\tau_1, \ldots, \tau_N)$, $R - \frac{\hbar}{2}\tau = (\mathbf{r}_1 - \frac{\hbar}{2}\tau_1, \ldots, \mathbf{r}_N - \frac{\hbar}{2}\tau_N)$ and $\tau P = (\tau_1\mathbf{p}_1 + \ldots + \tau_N\mathbf{p}_N)$.

In the general case, the mixed representation $F(R,P,t)$ can be used to derive separate distributions over coordinates and over particle momenta

$$F_R(R,t) = \int F(R,P,t)\mathrm{d}P, \tag{17}$$

$$F_P(P,t) = \int F(R,P,t)\mathrm{d}R.$$

Using the Wigner density matrix, the average value of any operator $\hat{T}(R,P)$ depending on R and P is calculated from the formula

$$\langle\hat{T}\rangle = \int \mathrm{d}R\mathrm{d}P\hat{T}(R,P)F(R,P). \tag{18}$$

Thus, the mixed representation for the density matrix (16) is similar to the ordinary distribution function used in classical statistical mechanics; its standard expressions can be employed to find the average values of physical quantities. There is, however, one fundamental difference between the classical and quantum descriptions: unlike the classical distribution function of particles over coordinates and momenta, the density matrix $F(R,P,t)$ can acquire not only positive but also negative values. This is due to the fact that the function $F(R,P,t)$ has no clear physical meaning because it is known that particle coordinates and momenta cannot be measured simultaneously in quantum mechanics. Only the distribution functions $F_R(R,t)$ and $F_P(P,t)$ have a physical meaning; they are positive.

The Liouville quantum equation (15) in the mixed representation has the form

$$\left(\frac{\partial}{\partial t} + \sum_{i=1}^N \frac{\mathbf{p}_i}{m}\frac{\partial}{\partial\mathbf{r}_i}\right)F_{\sigma',\sigma}(P,R) = = \frac{1}{i\hbar}\int\frac{\mathrm{d}\tau}{(2\pi)^3}\sum_{i\neq j}\int \mathrm{d}\mathbf{p}_i'\mathrm{d}\mathbf{p}_j'\delta(\mathbf{p}_i' + \mathbf{p}_j' - \mathbf{p}_i - \mathbf{p}_j) \times \times \exp\left\{\frac{1}{2}i\tau[(\mathbf{p}_i' - \mathbf{p}_j') - (\mathbf{p}_i - \mathbf{p}_j)]\right\}\left[u\left(\left|\mathbf{r}_i - \mathbf{r}_j + \frac{1}{2}\tau\hbar\right|\right) - u\left(\left|\mathbf{r}_i - \mathbf{r}_j - \frac{1}{2}\tau\hbar\right|\right)\right] \times \times F_{\sigma',\sigma}(\mathbf{r}_1, \ldots, \mathbf{r}_N, \mathbf{p}_1, \ldots, \mathbf{p}_{i-1}, \mathbf{p}_i', \mathbf{p}_{i+1}, \ldots, \mathbf{p}_{j-1}, \mathbf{p}_j', \mathbf{p}_{j+1}, \ldots, \mathbf{p}_N, t). \tag{19}$$

The N-particle equation (19) can be transformed by standard quantum-mechanics methods [160] into a sequence of engaged equations for one-, two- and many-particle distribution functions. Thus, for one-particle distribution function, after integration over coordinates and spin variables of particles 2, 3, ..., N, we have

$$\left(\frac{\partial}{\partial t} + \frac{\mathbf{p}_1}{m}\frac{\partial}{\partial\mathbf{r}_1}\right)F_{\sigma_1',\sigma}(\mathbf{r}_1,\mathbf{p}_1,t) = \frac{1}{i\hbar}\frac{1}{(2\pi)^3}\left(\frac{N}{V}\right) \times \times \int \mathrm{d}\tau\mathrm{d}\mathbf{r}_2\mathrm{d}\mathbf{p}_2'\mathrm{d}\mathbf{p}_1'\sum_{\sigma_2}\exp[i\tau(\mathbf{p}_1' - \mathbf{p}_1)] \times \times \left[u\left(\left|\mathbf{r}_1 - \mathbf{r}_2 + \frac{1}{2}\tau\hbar\right|\right) - u\left(\left|\mathbf{r}_1 - \mathbf{r}_2 - \frac{1}{2}\tau\hbar\right|\right)\right] \times \times F_{2\sigma_1',\sigma_2',\sigma_1,\sigma_2}(\mathbf{r}_1,\mathbf{r}_2,\mathbf{p}_1,\mathbf{p}_2,t). \tag{20}$$

The equation for a two-particle function $F_{2\sigma_1',\sigma_2',\sigma_1,\sigma_2}(\mathbf{r}_1,\mathbf{r}_2,\mathbf{p}_1,\mathbf{p}_2,t)$ is more cumbersome.

The possibility of solving Eqn (20) is related to the choice of an appropriate approximation for the two-particle distribution function. Here we consider the simple self-consistent field approximation in which the two-particle function F_2 is represented as a product of one-particle functions

$$F_{2\sigma_1',\sigma_2',\sigma_1\sigma_2}(\mathbf{r}_1,\mathbf{r}_2,\mathbf{p}_1,\mathbf{p}_2,t) = F_{1\sigma_1',\sigma_1}(\mathbf{r}_1,\mathbf{p}_1,t)F_{1\sigma_2',\sigma_2}(\mathbf{r}_2,\mathbf{p}_2,t). \tag{21}$$

Let us introduce a density matrix normalised to the density of the number of particles

$$f_{\sigma',\sigma}(\mathbf{r},\mathbf{p},t) = \frac{N}{V}F_{1\sigma_1',\sigma_1}(\mathbf{r}_1,\mathbf{p}_1,t). \tag{22}$$

Then, in the self-consistent approximation, Eqn (20) for a steady-state case acquires a simple form [153] (the summation is done over spin variables)

$$\frac{\mathbf{p}}{m}\frac{\partial f(\mathbf{r},\mathbf{p})}{\partial \mathbf{r}} = \frac{1}{i\hbar}\frac{1}{(2\pi)^3}\int_{-\infty}^{\infty} d\tau \int_{-\infty}^{\infty} d\eta [\exp i\tau(\eta - \mathbf{p})] f(\mathbf{r},\tau) \times \quad (23)$$

$$\times \left[u_{ef}\left(\mathbf{r} + \frac{1}{2}\tau\hbar\right) - u_{ef}\left(\mathbf{r} - \frac{1}{2}\tau\hbar\right)\right],$$

where $u_{ef}(\mathbf{r})$ is the effective self-consistent potential energy

$$u_{ef}(\mathbf{r}) = u_e(\mathbf{r}) + \int v_{el}(\mathbf{r}-\mathbf{r}')f(\mathbf{r}',\mathbf{p}')d\mathbf{r}'d\mathbf{p}', \quad (24)$$

u_e is the external potential acting on particles (electrons) and v_{el} is the energy of electron–electron interaction.

Now we consider the metal–vacuum interface. Let us assume that axis z is normal to the metal surface, which coincides with the plane $z = 0$ and that the electron–electron interaction is purely electrostatic (without allowance for exchange and correlation). In this case, the effective potential u_{ef} is determined by the self-consistent Poisson equation the solution of which in the unidimensional variant has the form

$$u_{ef}(z) = 4\pi e^2 \int_{-\infty}^{z} d\xi q(\xi) \int_{-\infty}^{\xi} d\zeta q(\zeta), \quad (25)$$

where the electron density $\rho(z)$, appearing in the expression for the charge density

$$q(z) = n_+(z) - \rho(z) \quad (26)$$

is determined from the solutions of Eqn (23), while the density of ions $n_+(z)$ is considered specified. As usual, we shall assume that the density $\rho(z)$ is related to the function $f(z,\mathbf{p})$ by the equation

$$\rho(z) = \int f(z,\mathbf{p})d\mathbf{p}. \quad (27)$$

Since the effective potential acting on electrons does not depend on the coordinates x and y, then

$$u_{ef}\left(\mathbf{r} + \frac{1}{4}\tau\hbar\right) = u_{ef}\left(z + \frac{1}{4}\tau\hbar\right),$$

where $\tau = \tau_z$. The function $f(\mathbf{r},\mathbf{p})$ does not depend on the coordinates x or y either. Therefore, the left-hand and the right-hand parts of equality (23) can be integrated over the variables η_x, η_y, τ_x, τ_y, p_x and p_y. After integration, we have

$$\frac{p}{m}\frac{\partial f(z,\mathbf{p})}{\partial z} = \frac{1}{2\pi i\hbar}\int_{-\infty}^{\infty} d\tau d\eta [\exp i\tau(\eta - \mathbf{p})] f(z,\eta) \times \quad (28)$$

$$\times \int_{z-\frac{1}{2}\tau\hbar}^{z+\frac{1}{2}\tau\hbar} dy \int_{-\infty}^{y} q(x)dx.$$

Here, $\tau = \tau_z$, $\eta = \eta_z$ and $p = p_z$.

Solution of Eqn (28) can be found by standard methods of the kinetic theory, for example, by using the well-developed method of moments. Roldughin and Martynov have shown [153] how an equation for the electron density near the surface can be derived from Eqn (28). A number of asymptotic dependences can be derived in this way. For example, for the density of electrons in a metal far from the surface, Friedel oscillations were found

$$\rho(z) = n_+ + A\frac{\sin[2p_F(z+z_0)/\hbar]}{(2p_F z/\hbar)^2}, \quad (29)$$

where A is a coefficient, p_F is the Fermi momentum. In a vacuum at $z \to \infty$, we have

$$\rho(z) = B\exp\left(-\frac{z}{R_s}\right), \quad (30)$$

where B is a coefficient, R_s is a typical length of the attenuation of the electron density near the surface.

Comparison of the results obtained by the method of quantum distribution functions with the results of calculations by the density functional method in the same approximation shows [153] that the method of quantum distribution functions provides more precise and detailed information on the electron density distribution in metals. In particular, it describes the Friedel oscillations and predicts a steeper decay of the electron density near the metal surface where the simple exponential variation of the charge density *vs.* distance to the surface is established only asymptotically, which has a clear physical meaning.

3. Phenomenological method

Many properties of electronic systems the thermodynamic characteristics of which are substantially influenced by the surface can be determined using a simpler method which we would conventionally call the phenomenological method. This technique was used to calculate the disjoining pressure (see below) in thin films of liquid metals [161] and to determine the chemical potential of electrons in small particles.[162] An interesting feature of this method is the fact that the shift of the chemical potential of electrons is determined, as a first approximation, only by the surface to volume ratio for the object. The geometrical shape of the system and the contribution of the quantisation of energy levels manifest themselves in higher approximations.[161]

The method is based on the relationship between the density of electronic states $\rho(E)$ (E is the energy of electrons) and the Green function $G(\mathbf{r},\mathbf{r}',E)$ [163]

$$\rho(E) = \frac{1}{\pi}\,\mathrm{Im}\int G(\mathbf{r},\mathbf{r}',E)_{\mathbf{r}=\mathbf{r}'}d\mathbf{r}. \quad (31)$$

Electrons are considered to move in some self-consistent field. The presence of this field is taken into account by introduction of effective boundary conditions for the electron wave function or the Green function

$$\frac{\partial G(\mathbf{r}_s,\mathbf{r}')}{\partial n} - \lambda_s G(\mathbf{r}_s,\mathbf{r}') = 0. \quad (32)$$

where $\mathbf{r}_s$ is a vector belonging to the particle (or film) surface, $\mathbf{n}$ is an internal normal to the surface, λ_s a parameter of the theory which can be interpreted as the reciprocal of the thickness of the electron cloud near the metal surface. In order to find the parameter λ_s, one has to solve the problem of electron density distribution near the particle or film surface by one of the methods described above.

The Green function can be found from the equation [164]

$$\Delta G(\mathbf{r},\mathbf{r}',E) + k^2 G(\mathbf{r},\mathbf{r}',E) = -\delta(\mathbf{r}-\mathbf{r}'), \quad (33)$$

where

$$k = \sqrt{\frac{2m}{\hbar^2}(E + i\gamma)},$$

γ is the width of the energy levels of electrons, which can be related to lattice vibrations and other factors, $\delta(\mathbf{r}-\mathbf{r}')$ is a delta function.

A method for finding the Green function $G(\mathbf{r},\mathbf{r}',E)$ and the density of states $\rho(E)$ has been proposed by Balian and Bloch,[164] who found them as an expansion in terms of 'multiple scattering' of electrons by the surface. The Green function was represented as the sum

$$G(\mathbf{r},\mathbf{r}',E) = G_0(\mathbf{r},\mathbf{r}',E) + G_1(\mathbf{r},\mathbf{r}',E). \quad (34)$$

Here $G_0(\mathbf{r},\mathbf{r}',E) = [\exp(ik|\mathbf{r}-\mathbf{r}'|)]/4\pi|\mathbf{r}-\mathbf{r}'|$ is the Green function for free electron gas and $G_1(\mathbf{r},\mathbf{r}',E)$ is a correction to this function; it was proposed to determine the correction as the potential of a simple layer

$$G_1(\mathbf{r},\mathbf{r}',E) = \int_S dS_\alpha G_0(\mathbf{r},\boldsymbol{\alpha},E)\mu_1(\boldsymbol{\alpha},\mathbf{r}'). \quad (35)$$

The parameter $\boldsymbol{\alpha}$ used here and $\boldsymbol{\beta}$, $\boldsymbol{\gamma}$, and $\boldsymbol{\delta}$ used in the subsequent formulae are the coordinates of points in the layer and $\mu_1(\boldsymbol{\alpha},\mathbf{r}')$ is a

function characterising this layer. The derivative of the potential of the simple layer along the normal to the surface satisfies the equation

$$\frac{\partial G_1^{(+)}(\boldsymbol{\beta},\mathbf{r}')}{\partial n_\beta} - \frac{\partial G_1^{(0)}(\boldsymbol{\beta},\mathbf{r}')}{\partial n_\beta} = -\frac{1}{2}\mu_1(\boldsymbol{\beta},\mathbf{r}'), \tag{36}$$

where the subscripts (+) and (0) at the Green function mean that these derivatives are calculated when $\mathbf{r}$ approaches the surface from the inside and directly on the surface (for $\mathbf{r} = \boldsymbol{\beta}$), respectively.

From Eqns (32), (34)–(36), one can derive integral equation for $\mu_1(\boldsymbol{\alpha},\mathbf{r}')$

$$\mu_1(\boldsymbol{\beta},\mathbf{r}') + 2\,\lambda_s\int_S \mathrm{d}S_\alpha G_0(\boldsymbol{\beta},\boldsymbol{\alpha})\mu_1(\boldsymbol{\beta},\mathbf{r}') = 2\left(\frac{\partial}{\partial n_\beta} - \lambda_s\right)G_0(\boldsymbol{\beta},\mathbf{r}') + \\ + 2\int_S \mathrm{d}S_\alpha \frac{\partial G_0(\boldsymbol{\beta},\boldsymbol{\alpha})}{\partial n_\beta}\mu_1(\boldsymbol{\alpha},\mathbf{r}'). \tag{37}$$

This equation can be solved rather simply.[164] The Green surface function $\Gamma(\boldsymbol{\alpha},\boldsymbol{\beta})$ is introduced; it is defined as the solution of the integral equation

$$\Gamma(\boldsymbol{\beta},\boldsymbol{\gamma}) + 2\,\lambda_s\int_S \mathrm{d}S_\alpha G_0(\boldsymbol{\beta},\boldsymbol{\alpha})\Gamma(\boldsymbol{\alpha},\boldsymbol{\gamma}) = \delta(\boldsymbol{\beta}-\boldsymbol{\gamma}). \tag{38}$$

By multiplying Eqn (37) by $\Gamma(\boldsymbol{\beta},\boldsymbol{\gamma})$ and integrating over S_β, we obtain an equation for $\mu_1(\boldsymbol{\alpha},\mathbf{r}')$ having the following form:

$$\mu_1(\boldsymbol{\beta},\mathbf{r}') = 2\int_S \mathrm{d}S_\beta\left(\frac{\partial}{\partial n_\beta} - \lambda_s\right)G_0(\boldsymbol{\beta},\mathbf{r}') + \\ + 2\int_S \mathrm{d}S_\beta\int_S \mathrm{d}S_\gamma\Gamma(\boldsymbol{\alpha},\boldsymbol{\beta})\frac{\partial G_0(\boldsymbol{\beta},\boldsymbol{\gamma})}{\partial n_\beta}\mu_1(\boldsymbol{\gamma},\mathbf{r}'). \tag{39}$$

This equation is solved by the iteration method; for relatively smooth surfaces, the iterative process rapidly converges.[164] This gives the series

$$\mu_1(\boldsymbol{\beta},\mathbf{r}') = 2\int_S \mathrm{d}S_\beta\left(\frac{\partial}{\partial n_\beta} - \lambda_s\right)G_0(\boldsymbol{\beta},\mathbf{r}') + \\ + 4\int_S \mathrm{d}S_\delta\int_S \mathrm{d}S_\beta\int_S \mathrm{d}S_\gamma\Gamma(\boldsymbol{\alpha},\boldsymbol{\beta})\frac{\partial G_0(\boldsymbol{\delta},\boldsymbol{\gamma})}{\partial n_\delta}\Gamma(\boldsymbol{\gamma},\boldsymbol{\beta})\left(\frac{\partial}{\partial n_\beta} - \lambda_s\right)G_0(\boldsymbol{\beta},\mathbf{r}') + \ldots, \tag{40}$$

when the λ_s value is constant, the Fourier transform (p-variable) of the function $\Gamma(\boldsymbol{\alpha},\boldsymbol{\beta})$ can be readily found

$$\hat{\Gamma}(p) = \frac{\sqrt{p^2 - k^2}}{\lambda_s + \sqrt{p^2 - k^2}}, \tag{41}$$

which allows the calculation of every term of the series in expansion (40).

After the Green function $G(\mathbf{r},\mathbf{r}',E)$ and the density of state $\rho(E)$ have been found, one can determine all thermodynamic characteristics of electrons in small particles and films.

4. Statistics of the electron energy levels in small particles

Yet another method suitable for determination of characteristics of the electrons in small particles is based on analysis of distribution of energy levels. A nanoparticle is never shaped like an ideal sphere. All methods used to prepare nanoparticles imply the presence of impurities on the surface. The distribution of impurities over the particle surface is not ideal either. As a result, it is impossible to calculate the energy levels with an inaccuracy substantially smaller than the distance between the levels. Kubo was the first to notice this.[165] He proposed that the energy levels be regarded as being randomly distributed; the average distance between them was specified to be

$$\Delta_\mu \approx \frac{E_F}{N},$$

where E_F is the energy of Fermi electrons in the particle and N is the number of electrons. The Kubo assumption is matched by the Poisson probability density for the distance Δ between the neighbouring levels

$$P(\Delta) = \frac{1}{\Delta_m}\exp\left(-\frac{\Delta}{\Delta_m}\right). \tag{42}$$

Kubo used this probability density to calculate the heat capacity and the magnetic susceptibility of small particles.

Later, Gor'kov and Elyashberg[166] pointed out that Kubo's results were erroneous. This conclusion was based on the results obtained by Wigner,[167, 168] who considered the statistics of nuclear energy levels and showed the presence of correlations between them. Wigner's results have been mathematically substantiated and the character of correlations between energy levels has been established.[169–171]

It was shown[169, 170] that, in terms of the type of transformations that leave the Hamiltonian for a system of particles invariant, three ensembles can be distinguished, each being characterised by its own statistics of the distribution of levels: (i) orthogonal ensemble — for a system with an integer spin invariant with respect to the inversions of time and space coordinates; (ii) symplectic ensemble — for random interactions of particles invariant with respect to time inversion and for a half-integral spin of the system; (iii) unitary ensemble — for systems not invariant with respect to time inversion.

The orthogonal ensemble appears in the presence of a weak external magnetic field, either weak or strong spin-orbital interaction and with an even number of electrons in the particle. The symplectic ensemble implies strong spin-orbital interaction, able to mix the levels corresponding to different spins of the system; the number of electrons in the system should be odd. The unitary ensemble describes systems occurring in a strong magnetic field.

The normalised distribution of N ordered energy levels for any of the three ensembles is determined from the equation[172]

$$W_\beta(E_1,E_2,\ldots,E_N) = C_\beta\exp\left(-\frac{\beta}{2}\sum_i E_i^2\right)\prod_{j<k}|E_j - E_k|^\beta, \tag{43}$$

where C_β is a normalisation factor,

$$\int\ldots\int W_\beta\,\mathrm{d}E_1\ldots\mathrm{d}E_N = 1, \tag{44}$$

and the parameter $\beta = 1$, 2 and 4 for the orthogonal, unitary and symplectic ensembles, respectively.

The physical properties of small particles depend on the distribution of the electronic energy levels located directly near the Fermi level. The distribution of these levels is found for the limit $N\to\infty$ by integration over a large number of levels (except for those located in the central region of the energy spectrum)

$$P_\beta(E_i\ldots E_{i+n}) = \\ = \lim_{N\to\infty}\int\ldots\int W_\beta(E_1\ldots E_N)\mathrm{d}E_1\ldots\mathrm{d}E_{i-1}\mathrm{d}E_{i+n+1}\ldots\mathrm{d}E_N. \tag{45}$$

In the central part of the spectrum, the absolute position of the level does not play any role, only the distribution of the gaps between the levels being significant

$$\Delta_1 = E_{i+1} - E_i,\ \Delta_2 = E_{i+2} - E_{i+1}\ldots\Delta_n = E_{i+n} - E_{i+n-1}. \tag{46}$$

The role of the distributions[173] $P_0(\Delta)$, $P_1(\Delta_1,\Delta_2)$, $P_2(\Delta_1,\Delta_2,\Delta_3)$, ... successively decreases because the use of higher approximations in the calculation of thermodynamic properties results only in the refinement of calculations done in the first approximation. Below we restrict our consideration to the first approximation. In this case, the densities of distribution of the levels in the three above-mentioned ensembles at small Δ are given by the expressions

$$P_{\mathrm{ort}}(\Delta) = \frac{1}{2}\pi\frac{\Delta}{\Delta_{\mathrm{m}}}\exp\left[-\frac{1}{4}\pi\left(\frac{\Delta}{\Delta_{\mathrm{m}}}\right)^2\right],$$
$$P_{\mathrm{sym}}(\Delta) = \left(\frac{8}{3\sqrt{\pi}}\right)^6\left(\frac{\Delta}{\Delta_{\mathrm{m}}}\right)^4\exp\left[-\frac{69}{9\pi}\left(\frac{\Delta}{\Delta_{\mathrm{m}}}\right)^2\right], \quad (47)$$
$$P_{\mathrm{un}}(\Delta) = \frac{32}{\pi^2}\left(\frac{\Delta}{\Delta_{\mathrm{m}}}\right)^4\exp\left[-\frac{4}{\pi}\left(\frac{\Delta}{\Delta_{\mathrm{m}}}\right)^2\right].$$

The corresponding curves are shown in Fig. 1, which also presents the density of probabilities for the Poisson law. It can be seen that real distribution laws substantially differ from the Poisson law; the difference is that the density of distribution of levels for real systems tends to zero when $\Delta \to 0$. This means that the probability of finding closely located levels in small particles is exceptionally low; it is said that levels 'repel' one another. The repulsion of energy levels changes crucially the thermodynamic properties of small particles at low temperatures.

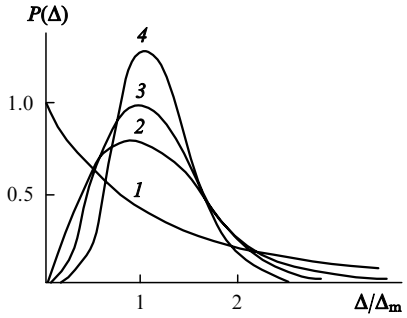


Figure 1. Probability densities for distances between the levels in the Poisson (*1*), orthogonal (*2*), unitary (*3*) and symplectic (*4*) ensembles.

IV. The electronic and thermodynamic properties of small metal particles and thin films

1. The electronic structure of small particles

As noted above, the density functional method is used most often to calculate the electronic structures of clusters and small particles (see reviews [174–176]). Even for clusters consisting of several atoms (and even in the absence of ligand shells), various approximations are used. The best known approximation is the jellium model, according to which a cluster is represented as consisting of two subsystems, namely, the positive charge distributed uniformly over the bulk, which models the ion core of the cluster, and delocalised electrons.

Calculations carried out within the framework of this model provide an explanation for the shell character of the electronic structure of atomic clusters of univalent metals. For 'bare' spherical clusters, single-electron energy levels correspond to the model of a spherically symmetrical potential well and form the sequence of states 1*s*, 1*p*, 1*d*, 2*s*, 1*f*, 2*p*, *etc*. Owing to the spherical symmetry, the energy states of electrons are degenerate, the degeneracy order being equal to $2(2l + 1)$ (with allowance for the electron spin). The numbers of electrons needed for the full occupancy of the shell can be easily found. They are 2, 8, 18, 20, 34, 40, *etc*. This sequence of filling the shells is matched by local extrema of the ionisation potentials of univalent metal clusters [175] (Fig. 2), although the jellium model does not reproduce the dependence of the ionisation potential of a cluster on its dimensions for a spherically symmetrical core. The mass spectrum of the most stable clusters corresponding to the so-called magic numbers cannot be reproduced in this model either. Note that clusters with closed electron shells, as shown by Brack,[176] are spherically symmetrical. The inadequacy of the spherical model for clusters with open shells is due to the deviation of the shape of these clusters from spherical. Calculations have been carried out [177, 178]

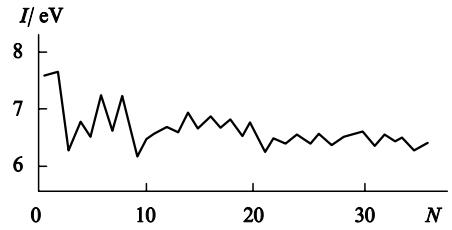


Figure 2. Ionisation potential (I) *vs*. the number (N) of atoms in the silver cluster.[175]

in which the distortion of the central field acting on the electrons was taken into account in the jellium model for clusters with partially occupied electron shells by replacing the spherical shape of the cluster by a spheroidal shape. The calculated characteristics of clusters, for example, of sodium clusters, such as the total energy, polarisability and ionisation potential follow a more complex dependence on the system dimensions than those in the spherical model and agree better with the experimental data.

A possible reason for the distortion of the spherical shape in the case of particles with non-filled electron shells has been established.[179] It is similar to the Jahn–Teller effect:[158] due to the high degeneracy of the quantum electron levels with respect to l, the energy of electrons in nearly spherical particles becomes a non-analytical function of the surface area of the cluster S. The change in the surface area upon the deformation of a spherical particle increases its surface energy, on the one hand, and decreases the energy of electrons due to splitting of the upper electron level E_{nl} (n is the principal quantum number), on the other hand. The resultant change in energy is found from the equation [179]

$$\delta E = \gamma\delta S - g(n,l,m_0)(\delta S)^{1/2},$$

where $g(n,l,m_0) > 0$ is a function of the principal and orbital quantum numbers and of the number of electrons m_0 in the outer shell, and δS is the change of the surface area of the particle upon deformation. The minimisation of the cluster energy determines the equilibrium deformation. According to an estimate made for cesium clusters, in the case of clusters with a size of 5 nm, the relative deformation can reach 10%. The same effect determines the size oscillations of the particle shape.

The possibility of a rearrangement of the ion core (not only of the change in the particle shape) also affects substantially cluster characteristics. Ivanov *et al*.[180, 181] carried out calculations for clusters in terms of the optimised jellium model they proposed. In this model, the distribution of the positive charge in the jellium was regarded as unknown *a priori* and was determined from the condition of the minimum total energy. The possibility of rearrangement of both the electronic energy spectrum and the ion core was assumed in the calculations. The calculations showed that the internal structure of a jellium-like core is formed in the cluster bulk and the positive charge is distributed non-uniformly in space. As a consequence, regions of maximum and minimum jellium density appear; they correspond to the equilibrium positions of ions in the lattice of a polyatomic cluster. The electron levels also rearrange, this effect being the most pronounced for clusters with filled shells. The magic numbers corresponding to the most stable electronic configurations of clusters with filled shells are also reproduced. For example, $N = 40$ is matched by the configuration $1s^2 1p^6 1d^{10} 2s^2 1f^{14} 2p^6$. The energy difference between optimised and non-optimised cluster models is 0.1 eV per atom and remains nearly constant for clusters with different sizes. The dependence of the average cluster radius on the number of atoms also changes substantially on passing from the non-optimised to the optimised model — this dependence becomes non-monotonic and local minima at $N = 8$, 20, 40, 58, *etc*. appear on the corresponding curve; *i.e*. clusters with filled shells are more compact.

The method of the density functional, including that as applied to clusters, can easily be extended to non-zero temperatures.[182–185] When the temperature differs from zero, Eqn (8) has the form

$$\rho(\mathbf{r}) = \sum_i \varphi_i^2 f(E_i - \mu). \quad (48)$$

Here,

$$f(E_i - \mu) = \left(1 + \exp\frac{E_i - \mu}{kT}\right)^{-1}, \quad (49)$$

μ is the chemical potential, k is the Boltzmann constant, T is temperature, and the function $f(E_i - \mu)$ should satisfy the condition

$$\sum_i f(E_i - \mu) = N, \quad (50)$$

where summation involves all the single-electron states.

For finite temperatures, Eqns (37) – (39) and (48) – (50) can be used to determine a single-electron energy spectrum of a system (*e.g.*, cluster), the electron density distribution in the system as well as the chemical potential and the occupancy numbers of electron states.

The temperature also influences substantially the structure of clusters. The distribution function of the levels located near μ changes markedly even at relatively low temperatures: it decreases for higher occupied levels and becomes non-zero for levels located above μ. The temperature variation of the occupancy numbers for 3*d*, 4*s* and 1*k* levels closest to the chemical potential level in the Na_{196} cluster has been calculated.[186] It was shown that the transition of electrons to higher energy levels starts even at temperatures appreciably (several times) lower than the values corresponding to the difference in energy between the levels. Moreover, at $T = 300$ K, the occupancy of the 1*k* level, which lies above the 4*s* level, proves to be greater than that of 4*s*. The pattern of variation of the chemical potential *vs.* temperature is equally complicated. In the clusters with $N = 18$, the chemical potential increases, while in clusters with $N = 40$, it, conversely, decreases with an increase in temperature. The complex temperature dependence of the chemical potential is due to the fact that it is determined by the orbital quantum numbers of the energy levels between which redistribution of electrons takes place.[186]

For finite temperatures, the deviation of the cluster shape from spherical is more significant than at $T = 0$ K. In the former case, the loss of sphericity can result not only from deformation of electron shells but also from thermal excitations of the ion core. However, the relevant calculations are associated with substantial procedural difficulties and have not been performed yet.

2. Thermodynamics of electrons in small particles

The thermodynamics of electrons in small particles have been studied fairly comprehensively by Denton *et al.*,[173] who calculated heat capacities and magnetic susceptibilities of particles for various ensembles. The thermodynamic characteristics of particles were found to depend on the number of electrons in them. The results of standard calculations with allowance for the level statistics are given in Table 1.

It can be seen from the Table that 'repulsion' of the energy levels changes in form the pattern of the temperature variation of the heat capacity of small particles. Instead of the linear dependence, typical of bulk samples,[187] a non-linear dependence correlated with the degree of repulsion of the levels is observed. The enhancement of the temperature dependence of heat capacity for low T values is due to the decrease in the probability of close arrangement of levels — the smaller the number of close levels, the smaller the number of electrons able to pass to higher levels on thermal excitation and the lower the heat capacity.

The difference between the heat capacities of particles with even and odd numbers of electrons is not as pronounced as the difference in the magnetic susceptibilities. For even numbers of electrons, the magnetic susceptibility tends to zero at $T \to 0$ for orthogonal and symplectic ensembles; this is explained by pairing of electrons on separated levels. In the case of the Poisson ensemble, the levels do not repel one another and, with a finite probability, they can be located rather closely; this results in a temperature-independent magnetic susceptibility. For systems with odd numbers of electrons, the magnetic susceptibility of any ensemble, conversely, tends to infinity. This pattern of susceptibility is due to the presence in the upper level of an unpaired electron, which accounts for the sharp increase in the susceptibility on a decrease in temperature.

Table 1. Heat capacities and magnetic susceptibilities of particles in various ensembles.

Ensemble	N is even	N is odd
Heat capacity (in k units)		
Poisson	$5.02(kT/\Delta_m)$	$3.29(kT/\Delta_m)$
Orthogonal	$3.02 \times 10(kT/\Delta_m)^2$	$1.78 \times 10(kT/\Delta_m)^2$
Symplectic	$3.18 \times 10^4(kT/\Delta_m)^5$	$1.64 \times 10^4(kT/\Delta_m)^5$
Unitary	$5.88 \times 10^2(kT/\Delta_m)^3$	$5.88 \times 10^2(kT/\Delta_m)^3$
Magnetic susceptibility		
Poisson	$3.04\left(\frac{1}{2}g\mu_B\right)^2/\Delta_m$	–
Orthogonal	$7.63\left(\frac{1}{2}g\mu_B\right)^2 kT/(\Delta_m)^2$	$\left(\frac{1}{2}g\mu_B\right)^2/kT$
Symplectic	$2.02 \times 10^3\left(\frac{1}{2}g\mu_B\right)^2 (kT/\Delta_m)^4/\Delta_m$	–

Note. Generally accepted designations: g is the gyromagnetic ratio, Δ_m is the average distance between electron levels.

Until recently, it has been impossible to verify these patterns of temperature dependence of the magnetic susceptibility and heat capacity by direct experiments because the systems prepared contained particles with both even and odd numbers of electrons. As a consequence, only ensemble-average characteristics were observed in experiments. It should be noted, however, that the magnetic susceptibilities of particles with even and odd numbers of electrons have been measured[3,4] in NMR experiments: the temperature dependence of susceptibility for particles with different numbers of electrons, even when they are present simultaneously in the system, can be determined from the Knight shift.

In recent years, substantial interest in the studies of the heat capacity and magnetic susceptibility of small particles has revived, which is due to the above-mentioned possibility of preparing metallic nanoparticles with a virtually definite number of atoms by the method developed in a series of studies.[78–89] The advances in the synthesis of nanoparticles permitted experimental verification of the correctness of the theory of their thermodynamic properties. Experiments of this type have been described by Volokitin *et al.*,[188,189] who carried out a detailed investigation of the thermodynamic characteristics of particles with different numbers of atoms (and, correspondingly, electrons). The experiments were performed with palladium clusters containing 561, 1415, 1740 and 2057 atoms as well as with larger clusters isolated from one another in the samples by ligand shells. The electronic heat capacity and magnetic susceptibility of metal particles were studied as functions of particle size and temperature in the range from 0.05 to 10 K, in which the effects of quantisation of the electron movement should be visible.

Figure 3 shows the temperature dependences of the specific heat capacity (C) of nanoparticles of various sizes and of bulk samples. It can be seen that the plots for nanoparticles of different sizes do not coincide at $T < 2$ K. The deviation from the data for bulk substances increases as the particle size decreases. The results of processing of experimental data by normalisation of the

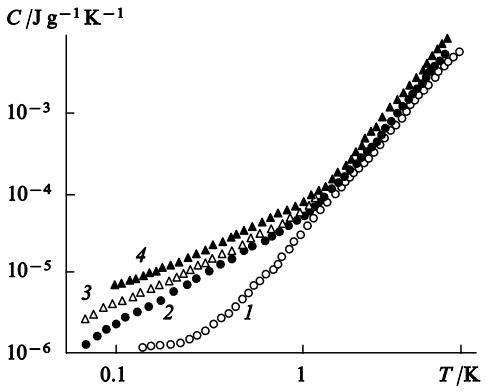


Figure 3. Temperature dependence of the specific heat capacity (C) for palladium clusters with five (*1*), seven (*2*) and eight (*3*) atomic shells and for clusters containing more than 10^5 atoms (*4*).[189]

dependences to characteristics of the particles of different dimensions are presented in Fig. 4. The same figure shows the theoretical $C(T)$ plot for the orthogonal ensemble. It can be seen from the figure that the theory reliably reproduces experimental data, which point unambiguously to quantisation of the electron levels in small particles.

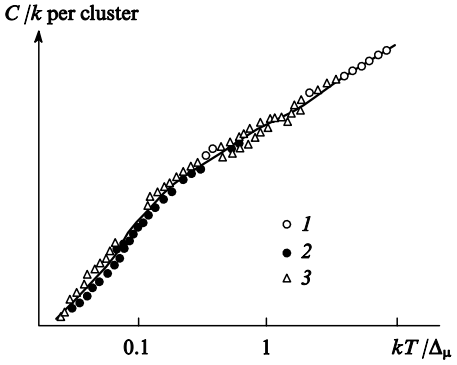


Figure 4. Normalised temperature dependences of the heat capacity for particles with different sizes.[189]
The continuous curve is the calculated dependence for the orthogonal ensemble.

Good agreement between theoretical and experimental results was also obtained for magnetic susceptibility measurements (Fig. 5). These experiments are actually the first studies in which

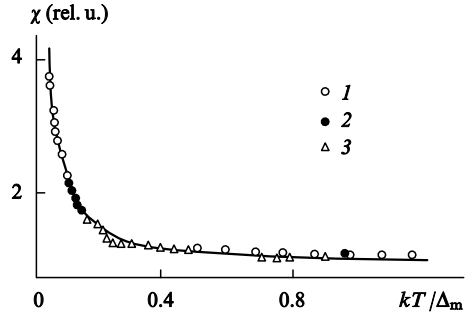


Figure 5. Normalised temperature dependences of the magnetic susceptibility (χ) for nanoparticles with five (*1*), seven (*2*) and eight (*3*) atomic shells.[189]
The continuous curve is the calculated dependence for the orthogonal ensemble with equal percentages (50%) of particles with even and odd numbers of electrons.

the quantum nature of electrons in small particles was demonstrated in an explicit form.

3. Disjoining pressure in liquid metallic films

The stability of free liquid films is due to a positive disjoining pressure $\Pi(H)$,[190] which prevents a decrease in their thickness H. The disjoining pressure $\Pi(H)$ is the difference between the pressure normal to the film surface and the pressure in the bulk phase contacting with the film.[190] The pressure difference arises due to the surface forces when the boundary layers of the two phases overlap.

It is commonly supposed[190] that the disjoining pressure in single-component systems is always negative; therefore, free films of neat substances cannot be stable. However, it has been shown[61, 191–193] that this rule can be violated for liquid metal films. The appearance of a positive component of disjoining pressure is related to the quantisation of the electron movement in thin films. The physical nature of this component of disjoining pressure is rather simple. According to the Heisenberg uncertainty principle, the component of the electronic momentum directed at the right angle to the surface cannot be smaller than $\hbar/H$. As a consequence, the minimum possible energy of electrons in the film amounts to $\hbar^2/2mH^2$. Owing to this restriction, the energy of each electron in the film increases, due to degeneracy, by a value approximately equal to the above value, even for a continuous spectrum of electron energies. Thus, the change in the density of the total energy of electrons is

$$\Delta E \sim \frac{N\hbar^2}{2mH^2V},$$

where N is the number of electrons in the film and V is the film volume. The pressure of the degenerate electron gas is proportional to the energy density. As a result, the pressure of electrons in thin films increases with respect to the pressure in the bulk by the value

$$\Pi(H) \sim \frac{N\hbar^2}{2mH^2V}.$$

The electron component of the disjoining pressure in thin films was calculated by two methods;[161, 192, 193] in one method, the model of a potential well with infinitely high walls was used, while the other method was based on the phenomenological model considered above in which the derivative of the electronic wave function on the film surface was specified. In the former case, the film was found to be absolutely stable, while in the latter case, film stability was determined by the nature of the surrounding medium. Let us consider results obtained by Roldughin and Deryagin.[161, 193] According to these studies,

$$\Pi(H) = E_{0\,\mathrm{F}}\frac{N}{V}R^2 \times \qquad (51)$$
$$\times \left[\chi_s(\lambda_s) + \frac{2}{R}\exp\left(-\frac{\gamma}{\sqrt{E_{0\,\mathrm{F}}}}\right)\sin\left(2\sqrt{\frac{2mE_{0\,\mathrm{F}}}{\hbar^2}}H + \varphi_0\right)\right],$$

where $E_{0\,\mathrm{F}}$ is the Fermi energy for a bulk sample

$$R = \frac{1}{H}\left(\frac{V}{3\pi^2 N}\right)^{1/3},$$

γ is a value characterising the width of electron levels[173] and $\chi_s(\lambda_s)$, φ_0 are functions of the parameter λ appearing in the boundary conditions. For the λ value corresponding to a potential well with infinitely high walls, expression (51) for $\Pi(H)$ transforms into the relation derived in another publication.[192] The function χ can be both positive and negative, its sign determining the sign of the disjoining pressure. The last term in relation (51) is insignificant for determination of the film stability because it represents a rapidly oscillating value. This term is due to the discrete character of the electron levels in thin films.

Let us clarify the nature of the change of the sign of disjoining pressure in a thin film following the change in the parameter λ_s, which describes the behaviour of the electronic wave function and, hence, the electron density near the geometrical surface of the film. Actually, λ_s specifies the distance by which electrons are 'allowed' to go out into the external environment. If electrons can easily leave the geometrical surface of the film, their effective density in the film decreases. The decrease in the effective density diminishes the Fermi energy and, as a consequence, the pressure of electrons in the film. Thus, the quantisation effect mentioned above, which ensures a positive disjoining pressure, can be counterbalanced by a decrease in the electron density. This implies that the stability of liquid metallic films is determined to a large extent by the nature of the environment.

Experiments confirm this conclusion. For example, the stability of mercury films adjoining various organic liquids has been studied.[194, 195] It was found that in octane, mercury films exist for infinitely long periods, whereas in decane, the lifetime of the films does not exceed 1 min; the lifetime in toluene is $\sim$1 s.

V. Optical properties of small particles

Nanometer particles have unique optical properties, which are used both for scientific and practical purposes. The optical characteristics of these particles are determined by conventional spectroscopic methods;[3, 196] therefore, the vast majority of studies devoted to a particular method for the preparation of nanoparticles contain sections devoted to their absorption spectra. Optical spectra provide fundamental information on the electronic structure of small metal particles. In particular, investigation into optical spectra allows one to follow the variation of electronic properties on passing from bulk samples to small particles.

The unique optical properties of small particles are finding application in the design of optical filters, markers of biomacromolecules, reversible photosensitive monochromic glasses, optical switches and optical traps and for surface enhancement of Raman light scattering spectra.

Absorption spectra of small metal particles have an intense broad band which is missing from the spectra of bulk samples. This band is associated with the collective excitation of the conduction electrons (surface plasmons); its occurrence in the visible region results in a unique colour spectrum of dilute colloidal dispersions of noble, alkaline earth and rare earth metal particles.

The nature of plasmon absorption is fairly simple. Under the influence of the electric field of the incident radiation, the conduction electrons in the particle are displaced with respect to the positively charged ion core. This displacement is cooperative, *i.e.* the movement of electrons is phase matched. The displacement of electrons gives rise to a force which acts to return the electrons to the equilibrium position. The returning force is proportional to the displacement, as for a typical oscillator; therefore, one can speak about the presence of a natural frequency of cooperative oscillations of electrons in a particle. The coincidence of the natural frequency of the cooperative electron oscillations with the frequency of the external field gives rise to a resonance effect related to the excitation of natural oscillations of electrons. In accordance with the symmetry of the spatial size distribution, the resonance cooperative movement of electrons can be represented as an infinite set of separate modes, namely, dipole, quadrupole and other modes. The description of the cooperative movement of electrons in terms of quantum mechanics results in the notion of elementary excitations — plasmons having the energy $\hbar\omega_0$, where ω_0 is the natural frequency of cooperative oscillations. The lifetime of plasmons is short, it is about tens of femtoseconds.

Although the optical properties of nanoparticles are determined by quantum effects, they are well reproduced in terms of the Mie theory,[3, 196] in which the optical properties of spherical metal particles in dielectric matrices are interpreted within the framework of classical electrodynamics. The response of a particle is described by Maxwell equations and the corresponding boundary conditions. Optical resonance (Mie resonance) also appears in terms of the Mie theory, due to the cooperative excitation of the electron plasma. The properties of the particle material do not appear in the Mie theory in an explicit form; it is assumed that they can be described using the complex dielectric constant, as in the case of bulk solids.

The profile of the absorption band near the Mie resonance for a nanoparticle is a Lorentzian curve characterised by the position and width of the $\hbar\omega_0$ peak. For particles with a size much smaller than the radiation wavelength, the resonance frequency is described by the expression [196]

$$\omega_0 = \left(\frac{ne^2}{\varepsilon_0 m_e}\right)^{1/2} (2\varepsilon_m + 1 + \chi_{1i})^{-1/2}, \tag{52}$$

where n is the density of electrons, ε_0 is the electric constant, m_e is the effective mass of the conduction electrons, ε_m is the real part of the dielectric constant of the medium, and χ_{1i} is its component related to the band–band transitions in the particle.

It can be seen from Eqn (52) that the position of the resonance depends not only on the parameters of the conduction electrons but also on band–band transitions and electron–hole excitations.

The resonance width is determined by the relation [196]

$$\Gamma_{r0} = 2\varepsilon_2(\omega)\left[\left(\frac{\partial\varepsilon_1}{\partial\omega}\right)^2 + \left(\frac{\partial\varepsilon_2}{\partial\omega}\right)^2\right]^{-1/2}, \tag{53}$$

where $\varepsilon_1(\omega)$ and $\varepsilon_2(\omega)$ are the real and imaginary parts of the dielectric constant of the particle and ω is the current radiation frequency.

According to the Mie theory, starting from some size of the particles (about one-tenth of the radiation wavelength), the position and the width of the absorption band no longer depend on the particle size. However, a substantial shift of the resonance and the broadening of bands following a decrease in the particle size was observed in experiments.

The relevant theoretical models have been considered.[197] The greatest contribution to the variation of the position of the peak as a function of particle size is made by the changes in the average density of electrons in the particles, in the effective mass of electrons and in the susceptibility related to the band–band transitions. However, for typical values of these parameters, the size corrections are usually too small. Therefore, it was assumed that for small particles, collisions of electrons with the surface of particles should be significant (the mean free path in gold is 20 nm). This hypothesis provided an interpretation of the spectra of relatively large particles (>3 nm for gold) but proved inapplicable to smaller particles. It is clear that the classical views on free electrons become invalid for small particles and quantum size effects should be taken into account. Nevetheless, no demonstrations of these effects have yet been identified unambiguously in the optical properties of small particles, although they show themselves in other properties;[175, 176] in particular, they are manifested as the change in the conductivity of single particles.[198, 199] This might be due to the use in experiments of particle ensembles having different sizes and shapes.

An attempt to overcome this difficulty has been undertaken by Alvarez *et al.*,[200] who studied the spectra of gold nanocrystals stabilised by n-alkanethiolates in toluene. The dimensions of metal particles varied from 1.4 to 3.2 nm (70 to 800 Au atoms); special methods for separation of narrow fractions of particles were used for this purpose. It was found that the absorption spectrum depends slightly on the length of the alkyl chain in the stabilising agent and that the characteristic band (2.4 eV) is broadened upon a decrease in the particle size and virtually disappears for 2 nm particles. A band corresponding to resonance transitions (1.7 eV) was identified and the presence of step structures in the absorption spectrum of small clusters (smaller

than 2 nm) was demonstrated. This spectral feature was attributed to the quantum size effects caused by transitions of electrons from the conduction bands to the discrete levels located above the Fermi level.

It should be noted in this connection that the assumption concerning the change in the optical parameters of gold for particles with a size of 3 nm has also been made previously.[201] It can be expected that 2 nm is an intermediate size in passing from continuous to atomic structure for particles passivated by thiolates. The transition of a nanoparticle to the metallic state is manifested especially clearly in the absorption spectra (see, for example, Refs 202 and 203).

For the width of the plasmon absorption band for nanoparticles, described by a continuum model, the following expression was obtained:[197]

$$\Gamma_r = \Gamma_{r0} + \frac{2\omega_0^2}{\omega^3} v_F \left[\left(\frac{\partial \varepsilon_1}{\partial \omega} \right)^2 + \left(\frac{\partial \varepsilon_2}{\partial \omega} \right)^2 \right]^{-1/2} \frac{A}{R}, \quad (54)$$

where v_F is the Fermi velocity of electrons, A is a constant, R is the particle radius.

The corresponding dependence of the width of the absorption band on the size of particles has been confirmed experimentally.[204] The magnitude of the constant A depends substantially on the nature of the medium surrounding the particles and on the presence and parameters of the adsorbates.[205] The medium or adsorbed molecules (electron donors or acceptors) can change markedly the effective concentration of electrons in the particle, resulting in a shift in the resonance and a change in the band width. Apart from this static shift of the resonance and the change in the width of the absorption band, dynamic effects related to the transfer of electrons from the Fermi surface to the adjacent levels of adsorbed molecules or the environment are also possible.

The effects of this type have been studied;[206–209] effects of adsorption of $S_2O_3^{2-}$ and halide ions on silver particles [206, 207, 209] and $S_2O_3^{2-}$ ions and pyridine molecules [208] on silver particles and on the particles of a copper–silver alloy in an aqueous solution were established. The resulting absorption spectra were processed in terms of the Mie theory; the concentration of conduction electrons in the particles and attenuation coefficients of plasmons were found as functions of adsorption of the corresponding ions. Experiments showed that for 3–5-nm silver and bimetallic particles, the concentration of conduction electrons increases by approximately 10% and 5%, respectively, and the absorption coefficient increases 2- and 1.6-fold, respectively. The increase in the electron density was explained by its movement from the adsorbate to the metal, while the increase in the attenuation coefficient was attributed to the increase in the cross-section of electron scattering on the surface defects which have captured the adsorbate molecules.

It should be mentioned that the Mie theory with appropriate modification of the parameters permits one to describe virtually all the available experimental data on absorption spectra (naturally, except for those for very small particles).[210] For this reason, theoretical description of the optical characteristics of particles lags substantially behind experimental studies. Simultaneously, the Mie theory has been developed to become more precise and more general in order to go beyond the limits of the approximations used. In particular, investigation into the influence of the shape and the state of the surface of particles on the optical properties have been started. In early studies, simple shapes of particles were chosen — spheres,[211–213] cylinders or parallelepipeds, because calculations were carried out by quantum-mechanics methods, which imposed certain demands on the shape of particles that enable exact solution of the Schrödinger equation. In these studies, electric absorption, stipulated by the electrical conductivity of particles (determination of which was the object of the studies), was calculated. In the case of particles with a size exceeding the mean free path of electrons, the conductivity is related to the bulk conductivity of the metal; hence, the calculation of electric absorption is actually reduced to determination of the electric field in the particle.

Magnetic absorption by spherical particles has been studied.[214] The calculations were based on the solution of the kinetic equation for electrons in terms of the Bhatnagar–Gross–Krook model. The same model was used in another study [215] to calculate the electronic and magnetic absorption of spheroidal particles. Particles with sizes both larger and smaller than the mean free path of electrons were considered. It was shown that the total absorption and the ratio of electronic to magnetic absorption depend appreciably on the shape of particles and polarisation of the incident electromagnetic wave; these values can change by several orders of magnitude with a fixed particle volume.

In the Mie theory and in other theoretical approaches, the particles are assumed to have a regular shape and smooth surface. However, in practice, this is not always true. In particular, clusters applied on a substrate are shaped like deformed spheroids rather than like spheres.[216] In addition, on the surface of particles, atoms can occupy positions with different coordination numbers; in particular, they can be rather low, which means roughness at the atomic level. As a result, new channels for light absorption by particles appear.

Experiments [217, 218] and theoretical calculations [219] showed that the state of the particle surface is really important for light absorption. Electron resonances localised in the near-surface layer are significant when they overlap with the surface plasmons. In this case, they are excited very rapidly because excitation of a plasmon is accompanied by enhancement of the field on the surface.

Absorption on the surface of small particles has been observed experimentally;[220] for this purpose, a special method for the separation of surface and bulk absorption was used. Metal particles shown [221] to have a smooth surface and surface electronic states were applied on a transparent substrate from the vapour phase at 100 K. The particles were exposed to pulse laser radiation, which excited the electrons on the surface and in the bulk. Upon attenuation of the excitations, the temperature of the sample rose, which caused desorption of atoms from the surface. The velocities of the desorbed atoms were measured in order to determine the temperature of the particles. From the difference between the temperatures, the energy absorbed by the particles was found. The surface and bulk excitations were separated by repeating this procedure for particles the roughness of which had been removed by heating and slow quenching. The experiments with sodium particles supported on the surface of quartz glass demonstrated that the surface contribution to the absorption is equal to 32% for clusters with a size of 21 nm.

In recent years, the interest in the optical properties of colloidal dispersions of bimetallic particles has markedly enhanced. Various pairs of metals have been studied.[222–227] Bimetallic particles containing silver and mercury received particular attention. Both metals are characterised by sharp absorption bands corresponding to surface plasmons and located rather closely together, *viz.* at 380 nm for silver in water and at 300 nm for mercury.[228] Bimetallic particles of this type having different compositions have been prepared.[229] Investigation of their absorption spectra showed that the plasmon resonance bands shift to shorter wavelengths as the content of mercury in the drops increases. The variation of the absorption spectra during the preparation of the colloids was studied. Mercury drops were found to be formed initially during the reduction of metals; silver ions are reduced simultaneously. Then an amalgam is formed in which silver particles occur in the drops of mercury. The colloid is stable if the Hg : Ag ratio is greater than 2. Otherwise, it starts to opalesce and sedimentation occurs. The formation of the amalgam influences the absorption spectrum: the plasmon resonance shifts towards longer wavelengths.

The non-linear optical properties of the nanoparticle ensembles proved unexpected; they are influenced by secondary cooperative effects caused by interaction of excited nanoparticles.

Abnormal enhancement of hyper-Rayleigh scattering in dispersions of gold nanoparticles has been observed.[230, 231] In a study of the influence of high radiation doses on silver nanoparticles, the presence of a limiting transmission threshold was established;[232] *i.e.* dispersion resulted in an increase in the light absorbance due to non-linear effects. This enhancement was attributed to photochemical processes which have started on the particle surface. Yet another cooperative effect was found in another study.[233] It was found that the intensity of the surface enhanced Raman scattering increases due to participation of surface ensembles of particles; this effect depends on the composition of particles in a rather complex manner (the experiments were carried out with nanoparticles of gold and silver).

VI. The influence of radiation on the stability of nanoparticles

The optical properties of nanoparticles can be changed by various types of treatment of the colloidal system, for example, by introducing stabilising or destabilising additives, by changing the temperature and also by irradiation of the system. A usual result of this types of treatment is the change in the aggregation state of the colloidal dispersion.

If the particles form aggregates,[234, 235] the corresponding plasmon band either shifts towards longer wavelengths or becomes broader. However, when the colloidal particles are aggregated, the distribution of particles in the aggregate does not correspond to a close packing. In most cases, aggregation yields fractal structures having one or another fractal dimension, depending on the aggregation conditions.[236–238] A theory of the optical properties of fractal clusters has been developed;[239, 240] it was shown that the presence of close neighbours of a particle in the aggregate changes the frequency of optical resonances of the particle and causes band broadening. The change in the frequency and band broadening are due to the dipole–dipole interactions between the light-induced dipole moments of particles. This effect underlies a method for the estimation of the degree of aggregation of colloidal systems, which allows one to monitor the evolution of colloids under complex conditions (see, for example, Ref. 202).

Hasegawa *et al.*[241] studied the light-induced variations in the stability of colloidal dispersions of ultrasmall particles. They investigated various metal particles dispersed in various organic media. It was found that a sol of gold in chloroform starts to sediment 4 h after irradiation by the light of a mercury lamp, whereas in the dark, it remains stable for a year. Thus, under the influence of light, the rate of coagulation increases by a factor of 1000.

Similar results were obtained for gold particles in water,[242] the rate of coagulation being dependent on the radiation frequency. The maximum rate was observed at the frequency corresponding to the Mie resonance. It has been suggested [243] that coagulation is caused by the dipole interaction of particles, which is enhanced by external radiation.

A more detailed study has been performed by Satoh *et al.*[13] The experiments were carried out with a gold sol prepared by vaporisation followed by deposition from the flow into an organic liquid without using surfactants or stabilisers. Gold sols in acetone, ethanol, propan-2-ol and chloroform as solvents were prepared. The changes in the absorption spectrum on exposure to the light of a mercury lamp and on heating the dispersion were determined. The initial peak (surface plasmon) at a wavelength of 523 nm was found to be broadened and to disappear; the band at 270 nm becomes more intense and a new band at 840 nm appears. The shift of the plasmon peak was attributed to the dipole–dipole interaction of particles in the aggregates.[234] After 20 h of irradiation, complete sedimentation of the aggregates occurred and redispersion was impossible. The rate of coagulation depended on the solvent used.

It was found by electron microscopy that nanoparticles form fractal aggregates with a dimension of 1.7, which corresponds to the diffusion-controlled aggregation model (at an initial stage, unidimensional chains are formed in the system). It was assumed that coagulation is due to the enhancement of the van der Waals attraction caused by the presence of induced dipoles. To verify this assumption, the effect of radiation with different wavelengths on the particles was studied. Coagulation was found to take place even on exposure to visible light. However, UV radiation markedly enhances coagulation. To explain the effect of the radiation wavelength on the rate of aggregation, it was suggested that the instability of the sol (in addition to the increase in the van der Waals interaction mentioned above), can also be related to the change in the Coulomb repulsion as a result of the change of the surface charge due to photochemical processes.

In order to verify this hypothesis, in addition to the measurements of the stability of a dispersion of gold particles in water and propan-2-ol under the action of radiation, their ζ potentials were measured.[14] The coagulation rate was determined not only from the shift of absorption but also by electron microscopy using a special procedure. The relationship between the rate of coagulation and the change in the ζ potential of the particle caused by the addition of a salt was studied. On exposure to radiation, the ζ potential decreased from -45 to -65 mV. The increase in the absolute magnitude of ζ indicates enhancement of the Coulomb repulsion between the particles; thus, this cannot account for the loss of stability of colloidal nanoparticles.

Karpov *et al.*,[244–246] who studied silver sols, proposed a somewhat different interpretation for photostimulated aggregation. The aggregation of particles was detected from the absorption spectra of colloids. It was established that the rate of aggregation increases by a factor of 10^{10} upon irradiation;[247] it was suggested that the acceleration of aggregation was based on the photoeffect.

The proposed mechanism is as follows. Irradiation of a colloid gives rise to oppositely charged particles, due to exchange of the electric charges arising upon photoemission. The exchange proceeds through the dispersion medium; it is due to the fact that the Fermi energy of particles depends on their size and results in equalisation of the electrochemical potentials of particles of different sizes. The long-range electrostatic forces arising after the exchange play a crucial role in the fact that particles approach one another to distances at which van der Waals forces start to show themselves.

The possibility of formation of a contact potential between quantum-size systems of the same nature has been indicated.[191, 192] This effect was attributed to the shift of the chemical potential under conditions where the movement of electrons is confined by the metal film surface. At the thermodynamic equilibrium, electrons are redistributed between systems of different sizes to ensure equal electrochemical potentials. The effect of this distribution of electrons between nanoparticles has been used [162] to introduce attractive forces between the particles in an equilibrated polydisperse system.

If the process of aggregation of nanoparticles is underlain by photoelectric emission, a 'red boundary' of the process should exist. The variation of the rate of photoaggregation of a silver hydrosol has been studied experimentally by exposure of identical samples to radiation in the range from 366 to 1050 nm.[246] The experiments showed that the rate of photoaggregation depends on the radiation wavelength and that a red boundary for the process does exist. However, when the radiation power is rather high, two-photon processes, which shift this boundary, start to play a noticeable role. An interesting feature of photoaggregation has been noted: a higher initial aggregation of particles implies a lower exposure dose required to increase aggregation by the same amount. In a freshly prepared sol, the process of photoaggregation does not start until a threshold radiation intensity is reached, because the sol does not contain spontaneously formed aggregates of two or three particles needed as seeds for photostimulated aggregation.[246]

The presence of a threshold irradiation dose in the process of destabilisation of colloidal silver sols has also been noted in another study,[93] in which irradiation was carried out by electrons (5 MeV) and γ-quanta (^{60}Co as the source). The irradiation by electrons was pulsed (pulse duration 2 μs). The coagulation of particles was indicated by changes in the optical absorption spectra. No changes were detected after 50 pulses. However, in the case of 60–70 pulses, the intensity of the major absorption band sharply decreased, while its width increased. An appreciable increase in the light scattering by the colloidal dispersion was also observed. A critical irradiation dose was also found to exist when γ-quanta were used. The loss of stability of sols in these experiments was attributed to the neutralisation of the particle charge due to the reduction of sorbed silver ions under the action of radiation; this destroys the double electric layer at the particle boundary. The specificity of the electron irradiation was in that it 'delivered' electrons, and the charge on the silver particle decreased upon absorption of these electrons. A similar view on the reasons for destabilisation of the nanoparticle sol on exposure to γ-radiation has been expressed in other studies;[248–251] regularities of the formation of fractal aggregates from silver nanoparticles have been investigated.[251]

VII. Relaxation of electrons in small particles

Direct measurements of the dynamics of electrons in small particles became possible, most of all, owing to the development of ultrafast laser equipment. Absorption spectroscopy is used most often. Short (100 fs) laser pulses are employed to bring electrons into excited states, the relaxation of which is observed by means of the second, probing laser beam. The dynamics of relaxation was determined from the time variation of the absorption between two successive excitations of the system. The variation of transparency with time, related to the restoration of the ground state of the system, is also measured in some cases. The dynamics of electrons in semiconductor particles has been considered in a review;[7] therefore, we do not discuss it here.

Metal particles differ substantially from semiconductor particles. The main difference is in the structure of electron energy levels. The forbidden gap, which plays a fundamental role in semiconductor particles, is lacking in the case of metals (Fig. 6). At ordinary temperatures, the distance between the electron levels in metal particles can be considered to be relatively small and their optical properties differ little from those of bulk metal samples.[175] Therefore, the electron dynamics in small metal particles markedly differs from that in semiconductor particles.

For small metal particles, only the optical absorption and structural properties have long been studied,[252–256] whereas the study of electron dynamics has started only recently. The regularities of electron relaxation for times longer than 2 ps have been elucidated.[257] The first femtosecond study of relaxation was performed by Roberti *et al.*[258] in relation to a dispersion of gold clusters in water. Subsequently, similar studies [259, 260] were carried out for silver and platinum nanoparticles in aqueous and organic media.

The investigations showed that for silver and gold particles, relaxation at early stages is determined by the electron–phonon interaction, the relaxation times being 2.5 and 7 ps, respectively. These times are longer than the corresponding relaxation times for bulk samples (670 fs for silver and 1 ps for gold).[261, 262] The retardation of electron relaxation in nanoparticles was ascribed [259] to the decrease in the electron–phonon interaction. This decrease has been predicted theoretically,[263] the relaxation time for gold particles corresponding to that measured for island films.[264] Similar femtosecond studies have been carried out for gold [265–270] and zinc [271] nanoparticles. Studies of gold particles in glass matrices resulted in a relaxation time of 4 ps.[266]

It was also demonstrated that the difference between the relaxation times for particles having the same size can be due to the use of different stabilising agents. Thus it was found [260] that the relaxation times for the same gold particles (18 nm) in water and cyclohexane are 7 and 3.5 ps, respectively.

For tin particles, the dependence of the relaxation time on the particle size was attributed [271] to the effect of electron collisions with the particle surface. These results stimulated investigations into this dependence for gold particles with strictly specified dimensions. Thus it was found [272] that the relaxation time (τ) for the Au_{55} particle is 1 ps and that for Au_{13} is 300 ps. The electron relaxation for the Au_{55} cluster with a diameter of 2 nm proceeds much faster than that in larger (14–40 nm) particles (Fig. 7), for which the relaxation time is 7 ps. The experimental results are described by a phenomenological formula [273]

$$\frac{1}{\tau} = \frac{aR^{\alpha}}{\tau_b} + \frac{bv_F}{R}, \qquad (55)$$

where a, b are constants, τ_b is the bulk relaxation time, v_F is the Fermi velocity, R is the particle radius and α is an integer which can be found from the corresponding theoretical model.[263]

According to Eqn (55), as the particle size decreases, the relaxation time first increases, because the first term (normalised electron–phonon interaction) predominates. When the particle size further decreases, the second term starts to predominate and the relaxation time diminishes.

The same pattern of variation follows from the measurements of electron relaxation in platinum particles.[273] However, the data for the Au_{13} clusters do not fit in this regularity. Thus, formula (55) is inapplicable to small clusters, apparently, due to the loss of metallic properties by the clusters (in particular, Au_{13}). This fact is also confirmed by measurements of the absorption spectra of these clusters,[272, 274] in which many new bands appear. From this it follows that the transition from bulk properties to molecular properties for gold clusters takes place in the range from 55 to 13 atoms.

Deviations from the dependence given by relation (55) are also observed upon an increase in the pumping radiation

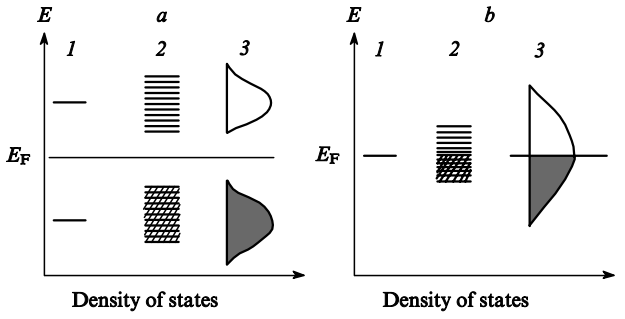


Figure 6. Diagrams of energy levels in semiconductors (*a*) and metals (*b*). (*1*) atoms, (*2*) small particles, (*3*) bulk samples. Occupied levels are cross-hatched, E_F is the Fermi level.

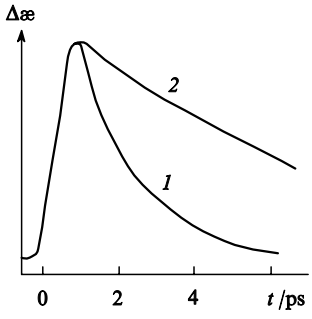


Figure 7. Change in the optical absorption coefficient (æ) *vs.* time for excited Au_{55} particles (*1*) and gold particles with a dimension of 15 nm (*2*).[272]

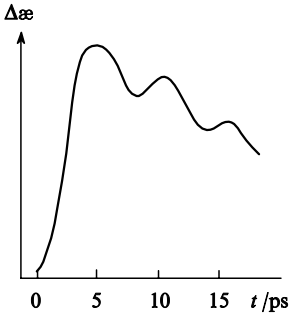


Figure 8. Change in the optical absorption coefficient *vs.* time for excited gold nanoparticles with a dimension of 15 nm.[270]

power.[268, 270, 275] In this case, the time of electron relaxation increases linearly with the intensity of the pumping radiation power, which is due to the heating of electrons and 'detachment' of their temperature from the temperature of the ion lattice.

Yet another interesting phenomenon was discovered in the studies cited above, namely, modulation of the absorption of the probing radiation (Fig. 8). The modulation was found for gold particles with a size from 14 to 17 nm. It was found that the modulation frequency did not correspond to the average gap between the electron levels

$$\Delta_m \approx \frac{E_F}{N},$$

the discreteness of which could, at the first glance, account for the modulation. For the particles studied, the modulation frequencies and the widths of energy gaps between the levels differ by an order of magnitude. Therefore, it was suggested [275] that these modulations are due to vibrations of the particles. Analysis shows [276] that the frequency of the acoustic vibrations of particles is close to the observed modulation frequency of the electron relaxation. The observed changes in the modulation frequencies and acoustic vibrations, depending on the particle size, are also consistent with experimental results.

Acoustic vibrations show themselves in the optical absorption spectra in the following way.[275] In conformity with the Mie theory,[196] the absorption coefficient of a particle is

$$æ(\omega) \propto \varepsilon_m^{3/2} \frac{\omega\varepsilon_2(\omega)}{[\varepsilon_1(\omega) + 2\varepsilon_m]^2 + \varepsilon_2(\omega)^2}. \quad (56)$$

The resonance absorption takes place when

$$\varepsilon_1(\omega) = -2\varepsilon_m.$$

In the free electron model,

$$\varepsilon_1(\omega) = 1 - \frac{\omega_0^2}{\omega^2 + \Gamma_e^2}, \; \varepsilon_2(\omega) = \frac{\omega_0^2\Gamma_e}{\omega(\omega^2 + \Gamma_e^2)}, \quad (57)$$

where Γ_e is the reciprocal relaxation time of electrons.

It can be seen from relations (52) and (57) that the position of the plasmon resonance depends on the density of electrons in the particle (because of a similar dependence of ω_0). As the electron density increases, the resonance shifts to shorter wavelengths; when the density decreases, it shifts to longer wavelengths. The possibility of this change in the position of the plasmon band was shown in experiments on pulse radiolysis [227] of identical silver particles with a size of 6 mm. As a result of vibrations of the ionic lattice, the electron density in the particles changes periodically, which shows itself as the periodic modulation of absorption.

In a study of electron relaxation in experiments similar to those described above,[266, 277] silver particles 40–60 nm in diameter and gold particles 15–20 nm in diameter were found to be broken to give smaller fragments (5–20 and 5 nm, respectively). The fragmentation was induced by the radiation from a pumping laser able to cause ionisation of the particles. The radiation power played a minor role. The fragmentation was due to the appearance of an electric charge on the particles upon photoemission.[266] This is confirmed by the fact that this effect was especially pronounced when the solution contained molecular traps for electrons.

VIII. Electron transfer through nanoparticles

Metal nanoparticles are unique objects to study the transfer of electrons through point contacts. For contacts between particles, non-linear current–voltage characteristics and (for low voltages) current suppression have been found.[278–282] In recent years, nanoparticles have started to be used in experiments with point contacts. The tip of a tunnelling microscope normally serves as one of the electrodes in these experiments (Fig. 9).[283–289] The intensive research along this line started after a single nanoparticle had been isolated and stabilised on a substrate.[27]

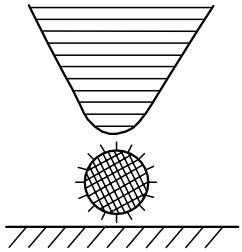


Figure 9. Scheme of the experiment on electron tunelling through individual particles.

The observed anomalies of current–voltage characteristics were attributed from the beginning [278] to the fact that an electron which skips from a particle to an electrode changes the particle charge by the magnitude of the electron charge e and thus increases the electrostatic energy by

$$\Delta E \approx \frac{e^2}{C},$$

where C is the capacitance of the particle. The capacitance of a spherical particle with the radius R coated by a shell with thickness d and having the dielectric constant ε in an electrolyte solution is found from the relation

$$C = 4\pi\varepsilon\frac{R}{d}(R + d).$$

For an electron to be able to skip (tunnel) from the particle to an electrode, the energy of the electron should be greater than ΔE. To ensure that the electron has the required energy, a relatively high voltage should be applied on the electrodes

$$U \approx \frac{e}{C}.$$

In experiments with single nanoparticles,[27, 289] several steps can be found in the current–voltage characteristics (Fig. 10, curve *1*). It was shown [282] that in the intervals between the steps, the particle charge does not change and is equal to e, 2e, 3e, *etc*. In addition, the conductivity of the electrode–particle system exhibits several maxima arranged at intervals (Fig. 11).

The maxima are due to degeneration of the electrostatic energy of the particle [290]

$$E(Q) = \frac{Q^2}{2C} + VQ \quad (58)$$

with respect to the charge Q; here V is the potential of the particle. The condition of the energy degeneration with respect to charge

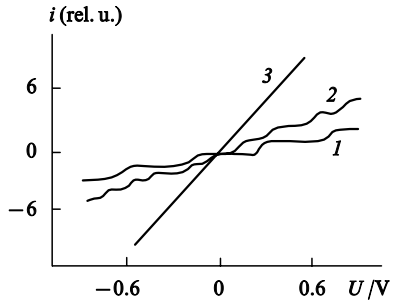


Figure 10. Current–voltage characteristics of a nanoparticle–electrode system for particles of different sizes increasing in the sequence $1 < 2 < 3$.

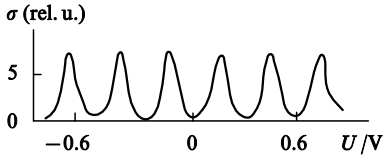


Figure 11. Electrical conductivity of a nanoparticle–electrode system *vs.* applied voltage.

$$E[(n-1)\mathrm{e}] = E(n\mathrm{e})$$

is fulfilled for the potential

$$V_n = -\frac{(2n-1)\mathrm{e}}{2C}. \qquad (59)$$

The effects of tunnelling through single particles have been studied fairly comprehensively by electrochemical methods.[287] Particles of different sizes were considered; in addition to experimental studies, data of numerical modelling of the processes occurring in the system shown in Fig. 9 were presented. In particular, transfer of electrons through the adlayer of the particles characterised by a particular size distribution was studied. It was shown that in the case of a particle ensemble of this type, the steps on the current–voltage characteristics are blurred and disappear with an increase in the particle size (see Fig. 10).

IX. Self-assembly of nanoparticles

Metal nanoparticles meant for the use as elements of electronic devices should finally be deposited on substrates. The properties of ensembles of deposited particles depend appreciably on their distribution over the substrate; this problem has drawn considerable attention. The possibility of deposition of ordered structures consisting of nanoparticles is of special interest; they can serve as miniature electronic devices: memory elements, lasers, screens, switches, *etc*. These ordered structures have been called quantum dots.[291–293]

The periodic structures based on nanoparticles were initially prepared by deposition of atoms on specially prepared substrates. For example, a procedure for the preparation of ordered islands of silver on the Pt(III) surface has been described.[294] The islands were formed as a result of nucleation of silver atoms on a substrate surface with a pre-formed structure of separate silver atoms. It is clear, however, that this procedure is applicable only to a very narrow range of materials; therefore, the search for new, more versatile methods for the preparation of ordered structures from nanoparticles continues. A possible approach is deposition of clusters grown beforehand.

The method of targeted deposition of clusters was apparently implemented for the first time by Fucks *et al*.[295] Low-energy monodisperse clusters obtained from the gas phase were deposited *in vacuo* on a substrate. Cluster sub-monolayers containing several tens to several thousands of atoms were prepared in this way. Observations showed that these clusters are not destroyed when brought in contact with a solid support. For big clusters, diffusion coefficients over the surface are low; therefore, the clusters do not migrate over the surface, their coalescence also being largely suppressed. As clusters are accumulated on the substrate, peculiar structures corresponding to successive deposition of strongly fixed particles are formed.

The resulting films are highly porous and are formed from aggregates of nanoclusters having a fractal structure similar to that found for particles in thin polymeric films.[237,238] The fractal dimension and characteristic size of the aggregates are determined by the regime of cluster deposition on the substrate.

It has been proposed [296] to deposit energy-charged clusters; in this case, characteristics of the structures formed can be varied over wider limits. The process of formation of structures from deposited clusters was also modelled in numerical experiments. Experimental data and the results of modelling have been surveyed in reviews.[297,298]

Ordered structures consisting of nanoparticles supported on substrates are of the greatest interest. These structures were first obtained using self-assembled monolayers of surfactants and resorting to the lithography methods. It has been shown [299–306] that deposition of surfactant monolayers followed by treating them with beams of low- or high-energy electrons or ultraviolet radiation and the use of scanning tunnelling microscopy affords ordered structured layers of metal particles with characteristic dimensions of up to 20 nm. Periodic structures of metal nanoparticles have also been prepared [307] by deposition of a metal on a substrate coated by an ordered adlayer of inert particles with sizes from 50 nm to 30 mm. In this case, the metal is applied on the substrate through the spaces between the inert microparticles.

In recent years, considerable progress has been made in the development of a method that implies formation of ordered nanostructures (colloid crystals) directly from nanoparticles formed in colloidal solutions. The attraction of this method is that it provides the possibility of varying the particle size over wide limits, the structure of the particles being controlled quite reliably by advanced techniques. In addition, the ligand or adsorption shell and, hence, the electronic properties of the particles can be varied as desired. Finally, successful use of this method hardly depends on the nature of the particles.

A method for the preparation of colloid crystals was first realised for CdS nanoparticles.[308] The procedure of evaporation of a solution from a colloidal dispersion film was used. During evaporation, either homogeneous or heterogeneous (on the substrate) nucleation of colloid crystals takes place. By this method, one can form both three- and two-dimensional colloid crystals. The scheme of deposition of ordered nanostructures is presented in Fig. 12 The resulting structures were studied by electron microscopy, which showed the presence of nanocrystals with ordering in the range of about 50 μm.

Subsequently, this method has been widely used to prepare ordered structures from metal nanoparticles.[31,48,309–319] Initially, the experiments were carried out with gold nanoparticles because in this case, the composition of the particles was constant and the

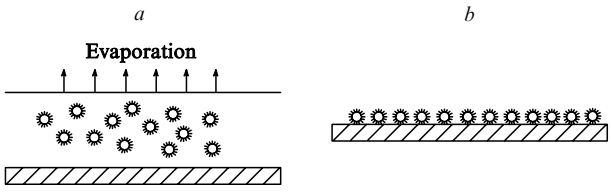


Figure 12. Scheme of the formation of ordered structures from nanoparticles by evaporation of the solvent.
System: (*a*) before evaporation; (*b*) after evaporation.

ligand shell formed from alkanethiols was sufficiently stable to ensure high stability of the colloidal dispersion and a colloid crystal. In addition, gold nanoparticles coated by an alkanethiol adlayer permit easy replacement of the solvent; the nanoparticles can be deposited and again dispersed and exchange reactions with the ligand environment can be carried out.

It has been demonstrated in various studies that nanoparticles form either a planar hexagonal structure or crystals with an FCC lattice. Detailed investigations dealing with the structure of colloid crystals and its dependence on the structure of nanoparticles have been carried out.[19, 20, 320] It was found that in the case of ordered multilayer structures, a colloid crystal necessarily has the (111) face. This was explained by the important role of the surface forces in the formation of colloid crystals because in ordinary crystals, this face has the minimum surface energy.

The lattice of a colloid crystal formed by gold nanoparticles and stabilised by quaternary ammonium bromides with alkyl radicals of various lengths has been studied.[319] It was found that the lattice parameter of the colloid crystal depends linearly on the length of the hydrocarbon radical. When the second layer of nanoparticles is deposited, they form either linear or ring structures on the hexagonal lattice formed by the first layer. The particles in the second layer occupy preferentially the sites above the contact points of the first-layer particles.

Characteristic features of the packing of particles have also been studied for the colloid crystals of gold[200] and silver[321] stabilised by alkanethiols. In this case, too, a correlation was established between the length of the alkyl chain and the lattice parameter of the colloid crystal. In addition, it was found by the method of chemical imaging in transmission electron microscopy with electron energy filtering[321] that the alkyl 'tails' of the adlayer of one particle penetrate rather deeply into the adlayers of neighbouring particles and form a sort of chemical bond with them. These experimental data confirm the results of molecular dynamics modelling of the behaviour of long-chain alkanethiols on the surface of nanocrystals.[322]

The interaction between silver nanoparticles coated by thiolates and forming ordered structures has been studied in detail.[323] The aggregation of nanoparticles and the structural transitions in thin layers and in the bulk of the colloidal solution were investigated. By comparing the experimental data with the results of numerical modelling, parameters of the particle–particle interaction were determined for the van der Waals attraction and for the short-range repulsion. It was shown that model of 'soft spheres' is the most adequate model for nanoparticles. A more comprehensive theoretical study of the characteristic features of nanoparticle structurisation at interfaces has been carried out by Gelbart *et al*.[324]

For the preparation of colloid crystals by vaporisation, the monodispersity and the shape of particles and the nature of the stabilising shell are significant. Self-assembly of gold, silver and platinum nanoparticles has been studied.[51] Nanoparticles were first prepared in water and then transferred into organic solvents containing thiolates; thus, the particle size and shape could be varied over wide limits. All the systems studied displayed the capability of self-assembly. The effect of the stabilising agent on the preparation of colloid crystals from nanoparticles has been considered by Lin *et al*.,[325] who worked with gold nanoparticles synthesised in reverse micelles using various stabilisers containing thiol, amino and sulfide groups. It was found that the formation of colloid crystals proceeds most readily in the presence of ligands with thiolate groups. The use of dodecanethiol was found to be the most efficient; with this compound, colloid crystals are spontaneously formed, nanoparticles being spontaneously segregated according to their sizes.

Nanoparticles arranged in crystals exhibit new cooperative properties;[46, 326] in particular, for two-dimensional crystals, the plasmon band shifts towards lower energies with respect to that for isolated nanoparticles. This effect is more pronounced when three-dimensional colloid crystals are formed; in this case the profile of the absorption band also changes. This change in the band profile is due to the influence of the particle environment and to the tunnelling of electrons between them. The latter factor starts to be significant when the distances between the particles are close to 2 nm; the average distance between nanoparticles coated by, *e.g*., dodecanethiol is 1.8 nm.

The hypothesis concerning the influence of tunnelling on the absorption spectra has been verified;[327] for this purpose, the energy shift of the plasmon band and the coefficient of light reflection from self-assembled structures consisting of silver particles with various distances between the closest particles were studied. Experimental data were approximated by theoretical curves constructed using the Maxwell–Garnett model. As particles approach one another to distances of several nanometers, the optical characteristics change sharply and the discrepancy between the calculated and experimental data becomes more pronounced. A substantial deviation of the results obtained in terms of classical theory from experimental results was found for the non-linear susceptibility of nanoparticle crystals, which characterises the generation of the second optical harmonics.

The cooperative effects in self-assembled nanoparticles are so pronounced that it is possible to obtain structures exhibiting dichroism by special techniques.[328] It is even possible to control the optical characteristics of ordered layers of nanoparticles.[42] The relevant experiments were concerned with the regularities of light transmission through and light reflection from multilayer films consisting of isolated gold nanoparticles. The experiments were carried out under conditions where a potential was applied on the film (by injection of electrons). Both the reflectance and the transmittance changed upon application of the potential. It was found that the observed changes in the optical constants cannot be described in terms of the views on the individual behaviour of nanoparticles.

To promote self-assembly of nanoparticles into a supported crystal, special methods are used, for example, pre-treatment of the substrate,[329] which can consist in the preliminary formation of self-assembled monolayers (Fig. 13) the external part of which reacts efficiently with the particles or with their ligand environment; in this case, the nanoparticles are stabilised by complex surfactants having two functional groups selected according to the 'key–lock' principle (Fig. 14).

Langmuir–Blodgett films[46, 333] and electrophoretic deposition of nanoparticles[334, 335] have been used to design ordered structures of nanoparticles. Ordered structures of silver nanoparticles have also been prepared by thermal reduction of the

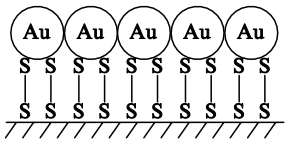


Figure 13. Scheme of the formation of ordered structures from nanoparticles on self-assembled monolayers.[330]

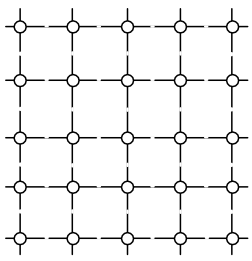


Figure 14. Scheme of the design of ordered structures from nanoparticles modified by surfactant vapours selected according to the 'key–lock' principle.[331, 332]

metal in a solution applied onto the surface of specially pre-treated mesoporous silica.[329] By using block copolymers which allow microphase separation, an ordered distribution of particles in films [336] and the formation of intricate structures from nanoparticles [337] can be attained. These structures can rearrange upon thermal treatment or upon introduction of additives influencing the microphase state of the block copolymer. Ordering of nanoparticles on a molten surface of a polymer the bulk phase of which remains solid has also been observed.[338]

Recent years have been marked by vigorous development of the methods for the preparation of self-assembled structures from nanoparticles with the use of biological objects: lipid tubes [339] or oligodesoxyribonucleotides containing terminal thiol groups,[340–342] which act as efficient organising agents in the case of gold nanoparticles. Biological systems permit several types of self-assembly of nanoparticles;[343] for example, the method found to be efficient for gold nanoparticles includes the use of streptavidin and biotin analogues. Biotin disulfide can be adsorbed on gold nanoparticles, which is followed by introduction of streptavidin; otherwise, biotin disulfide is bound to streptavidin and the complex is then adsorbed on the particles introduced. The complexity of this procedure is justified by the presence of a large number of biotin and streptavidin analogues and by the possibility of controlling the structure of the nanoaggregates synthesised and of preparing ordered structures of nanoparticles directly in solution.

X. Conclusion

The high practical value of nano-sized colloidal systems has stimulated substantial progress in their investigation in the last decade. Modern experimental equipment has enabled the preparation of individual nanoparticles with a specified size and the investigation of their properties. The advances in the synthesis and in the study of nanoparticles confirmed the theoretical models that had been developed decades ago but could not be verified because they were developed for ideal systems. It can be said that the high level achieved in the experiments on the preparation of nanoparticles is now close to the reachable limit. The methods used to investigate the properties of nanoparticles have also substantially improved. Almost exhaustive information on the structures of nanoparticles and on the electron dynamics in them was obtained. All this ensured transition to a new level of understanding of the physicochemical processes taking place in nano-sized colloidal systems.

However, the progress brought out new problems. The crucial role of the surface in the formation of properties of nanoparticles has become obvious. Nevertheless, the possibility of preparing nanoparticles with specified surface characteristics are still limited. The influence of the environment on the properties of nano-sized systems has not been adequately elucidated. There appeared the necessity of the development of theoretical approaches to the description of the properties of nanoparticles with intermediate sizes for which cooperative dynamics of electrons is replaced by the individual dynamics. New theoretical models describing the cooperative effects in nanoparticle ensembles including those taking into account the cooperation of their electronic component are required. At present, there are even no models which take into account the influence of the ligand (adsorption) shells when considering the dynamics of electrons in nanoparticles. In this respect, experimental research goes markedly ahead of the theory. However, experimental data now available constitute a good basis for the development of a more comprehensive theory of nanoparticle ensembles.

The author is grateful to Academician I I Moiseev, who initiated and stimulated writing of this review and to the Corresponding Member of the Russian Academy of Sciences Yu M Polukarov for reading the manuscript and making a number of useful remarks.

References

1. A I Gusev *Nanokristallicheskie Materialy, Metody Polucheniya i Svoistva* (Nanocrystalline Materials, Methods for Preparation and Properties) (Ekaterinburg: Institute of Chemistry of Solid, Urals Branch of the Russian Academy of Sciences, 1998)
2. H Gleiter *Nova Acta Leopoldina NF* **76** (303) 343 (1997)
3. Yu I Petrov *Klastery i Malye Chastits*y (Clusters and Small Particles) (Moscow: Nauka, 1986)
4. S A Nepiiko *Fizicheskie Svoistva Malykh Metallicheskikh Chastits* (Physical Properties of Small Metallic Particles) (Kiev: Naukova Dumka, 1985)
5. G B Sergeev, M A Petrukhina *Prog. Solid State Chem.* **24** 183 (1996)
6. A D Pomogailo *Usp. Khim.* **66** 750 (1997) [*Russ. Chem. Rev.* **66** 679 (1997)]
7. R F Khairutdinov *Usp. Khim.* **67** 125 (1998) [*Russ. Chem. Rev.* **67** 109 (1998)]
8. B C Gates *Chem. Rev.* **95** 511 (1995)
9. O Daub, W Langel, C Reiner, L Kienle *Ber. Bunsenges. Phys. Chem.* **101** 753 (1997)
10. H Abe, K P Charle, B Tesche, W Schulze *Chem. Phys.* **68** 137 (1982)
11. K Kimura, S Bandow *Bull. Chem. Soc. Jpn.* **56** 3578 (1983)
12. K Kimura *Bull. Chem. Soc. Jpn.* **60** 3093 (1987)
13. N Satoh, H Hasegawa, K Tsujii, K Kimura *J. Phys. Chem.* **98** 2143 (1994)
14. Y Takeuchi, T Ida, K Kimura *J. Phys. Chem. B* **101** 1322 (1997)
15. S Tohno, M Itoh *J. Aerosol Sci.* **24** 339 (1993)
16. S Tohno, M Itoh, H Takano *J. Aerosol Sci.* **25** S39 (1994)
17. S Tohno, M Itoh, S Aono, H Takano *J. Colloid Interface Sci.* **180** 574 (1996)
18. L Dimesso, S Humm, H Fuess, H Hahn *Ber. Bunsenges. Phys. Chem.* **101** 1750 (1997)
19. S A Harfenist, Z L Wang, M M Alvarez, I Vezmar, R L Whetten *J. Phys. Chem., B* **100** 13904 (1996)
20. S A Harfenist, Z L Wang, M M Alvarez, I Vezmar, R L Whetten *Adv. Mater.* **9** 817 (1997)
21. E D Shchukin, A V Pertsov, E A Amelina *Kolloidnaya Khimiya* (Moscow: Izd. Vyssh. Shkola, 1982)
22. G Schmid (Ed.) *Clusters and Colloids. From Theory to Applications* (New York, Weinheim: VCH, 1994)
23. M A Hayat (Ed.) *Colloidal Gold. Principles, Methods, and Applications* (New York: Academic Press, 1989)
24. N D Zhuravlev, V I Roldughin, A P Tikhonov *Kolloid. Zh.* **61** 322 (1999) [a]
25. L H Dubois, R G Nuzzo *Ann. Rev. Phys. Chem.* **43** 437 (1992)
26. H Giersig, P Mulvaney *Langmuir* **9** 3408 (1993)
27. M Brust, M Walker, D Bethell, D J Schiffrin, R Whyman *J. Chem. Soc., Chem. Commun.* 801 (1994)
28. M Brust, J Fink, D Bethell, D J Schiffrin, C J Kiely *J. Chem. Soc., Chem. Commun.* 1665 (1995)
29. R H Terrill, T A Postlethwait, C-h Chen, C-D Poon, A Terzis, A Chen, J E Hutchison, M R Clark, G Wingnall, J D Londono, R Superfine, M Falvo, C S Johnson Jr , E T Samulski, R W Murray *J. Am. Chem. Soc.* **117** 12537 (1995)
30. D V Leff, P C Ohara, J R Heath, W M Gelbart *J. Phys. Chem.* **99** 7036 (1995)
31. M J Hostetler, J J Stokes, R W Murray *Langmuir* **12** 3604 (1996)
32. R L Whetten, J T Khoury, M M Alvarez, S Murthy, I Vezmar, Z L Wang, P W Stephens, C L Cleveland, W D Luedtke, U Landman *Adv. Mater.* **8** 428 (1996)
33. A Badia, S Singh, L Demers, L Cuccia, G R Brown, R B Lennox *Chem. Eur. J.* **2** 359 (1996)
34. S R Johnson, S D Evans, S W Mahon, A Ulman *Langmuir* **13** 51 (1997)
35. M M Alvarez, J T Khoury, G Schaaf, M N Shafigullin, I Vezmar, R L Whetten *Chem. Phys. Lett.* **266** 91 (1997)
36. I Vezmar, M M Alvarez, J T Khoury, B E Salisbury, M N Shafigullin, R L Whetten *Z. Phys. D* **40** 147 (1997)
37. R J Arnold, J P Reilly *J. Am. Chem. Soc.* **120** 1528 (1998)
38. M J Hostetler, J E Wingate, C-J Zhong, J E Harris, R W Vachet, M R Clark, J D Londono, S J Green, J J Stokes, G D Wignall, G L Glish, M D Porter, N D Evans, R W Murray *Langmuir* **14** 17 (1998)

39. A C Templeton, S Chen, S M Gross, R W Murray *Langmuir* **15** 66 (1999)
40. S Chen, R W Murray *Langmuir* **15** 682 (1999)
41. S Chen *Langmuir* **15** 7551 (1999)
42. T Baum, D Bethell, M Brust, D J Schiffrin *Langmuir* **15** 866 (1999)
43. L A Porter Jr, D Ji, S L Westcott, M Graupe, R S Czernuszewicz, N J Halas, T R Lee *Langmuir* **14** 7378 (1998)
44. C K Yee, R Jordan, A Ulman, H White, A King, M Rafailovich, J Sokolov *Langmuir* **15** 3486 (1999)
45. F Bensebaa, T H Ellis, E Kruus, R Voicu, Y Zhou *Langmuir* **14** 6579 (1998)
46. J R Heath, C M Knobler, D V Leff *J. Phys. Chem. B* **101** 189 (1997)
47. K V Sarathy, G U Kulkarni, C N R Rao *Chem. Commun.* 537 (1997)
48. A Taleb, C Petit, M P Pileni *Chem. Mater.* **9** 950 (1997)
49. S Y Kang, K Kim *Langmuir* **14** 226 (1998)
50. A N Parikh, S D Gillmor, J D Beers, K M Beardmore, R W Cutts, B I Swanson *J. Phys. Chem. B* **103** 2850 (1999)
51. K V Sarathy, G Raina, R T Yadav, G U Kulkarni, C N R Rao *J. Phys. Chem. B* **101** 9876 (1997)
52. M Boutonnet, J Kizling, P J Stenius, G Maire *Colloids Surf.* **5** 209 (1982)
53. D Barnickel, A Wokaun *Mol. Phys.* **69** 1 (1990)
54. D Barnickel, A Wokaun, W Sager, H-F Eicke *J. Colloid Interface Sci.* **148** 80 (1992)
55. C Petit, P Lixon, M-P Pileni *J. Phys. Chem.* **97** 12974 (1993)
56. X M Lin, C M Sorensen, K J Klabunde, G C Hadjipanayis *Langmuir* **14** 7140 (1998)
57. J P Wilcoxon, P P Provencio *J. Phys. Chem. B* **103** 9809 (1999)
58. H Herrig, R Hempelmann *Mater. Lett.* **27** 287 (1996)
59. Ch Bruch, J K Krmger, H-J Unruch, W Krauss, B Zimmermaier, Ch Beck, R Hempelmann *Ber. Bunsenges. Phys. Chem.* **101** 1761 (1997)
60. V Cabra, V Pillai, B K Miskra *Langmuir* **11** 3307 (1995)
61. W Härtl, Ch Beck, M Roth, F Meger, R Hempelman *Ber. Bunsenges. Phys. Chem.* **101** 1714 (1997)
62. I Lisiecki, M P Pileni *J. Am. Chem. Soc.* **115** 3887 (1993)
63. I Lisiecki, M P Pileni *J. Phys. Chem.* **99** 5077 (1995)
64. I Lisiecki, F Billoudet, M P Pileni *J. Phys. Chem.* **100** 4160 (1996)
65. M P Pileni *Langmuir* **13** 3266 (1997)
66. M P Pileni *Ber. Bunsenges. Phys. Chem.* **101** 1578 (1997)
67. M P Pileni, T Gulik-Krzywicki, J Tanori, A Filankembo, J C Dedieu *Langmuir* **14** 7359 (1998)
68. C Tojo, M C Blanco, M A Lopez-Quintela *Langmuir* **13** 4527 (1997)
69. C Tojo, M C Blanco, M A Lopez-Quintela *J. Non-Cryst. Solids* **235**–**237** 688 (1998)
70. Y Li, C-W Park *Langmuir* **15** 952 (1999)
71. L Qi, J Ma, J Shen *J. Colloid Interface Sci.* **186** 498 (1997)
72. M Ji, X Chen, C M Wai, J L Fulton *J. Am. Chem. Soc.* **121** 2631 (1999)
73. A A Dokuchaev, T G Myasoedova, A A Revina *Khim. Vys. Energ.* **31** 353 (1997) [b]
74. A A Revina, E M Egorova, A D Karataeva *Zh. Fiz. Khim.* **73** 1897 (1999) [c]
75. Y Yu, S Chang, C Lee, C R C Wang *J. Phys. Chem. B* **101** 34 (1997)
76. M B Mohamed, K Z Ismail, S Link, M A El-Sayed *J. Phys. Chem. B* **102** 9370 (1998)
77. N T Tran, M Kawano, D R Powell, L F Dahl *J. Am. Chem. Soc.* **120** 10 986 (1998)
78. M N Vargaftik, V P Zagorodnikov, I P Stolyarov, I I Moiseev, V A Likholobov, D I Kochubey, A L Chuvilin, V I Zaikovsky, K I Zamaraev, G I Timopheeva *J. Chem. Soc., Chem. Commun.* 937 (1985)
79. M N Vargaftik, V P Zagorodnikov, I P Stolyarov, V A Likholobov, A L Chuvilin, V I Zaikovskii, D I Kochubei, G I Timofeeva, K I Zamaraev, I I Moiseev *Dokl. Akad. Nauk SSSR* **284** 896 (1985) [d]
80. M N Vargaftik, V P Zagorodnikov, I P Stolarov, I I Moiseev, D I Kochubey, V A Likholobov, A L Chuvilin, K I Zamaraev *J. Mol. Catal.* **53** 315 (1989)
81. L J de Jongh *Appl. Orgamomet. Chem.* **12** 393 (1998)
82. G Schmid, B Morun, J-O Malm *Angew. Chem., Int. Ed. Engl.* **28** 778 (1989)
83. G Schmid *Polyhedron* **7** 2321 (1988)
84. G Schmid, S Emde, V Maihack, W Meyer-Zaika, St Peschel *J. Mol. Catal. A, Chem.* **107** 95 (1996)
85. G Schmid *Chem. Rev.* **92** 1709 (1992)
86. B N Novgorodov, D I Kochubey, M N Vargaftik *Nucl. Instr. Meth. Phys. Res. A.* **405** 351 (1998)
87. V V Volkov, G van Tendeloo, M N Vargaftik, I P Stolyarov, I I Moiseev *Mendeleev Commun.* 187 (1993)
88. V V Volkov, G van Tendeloo, M N Vargaftik, I I Moiseev *J. Cryst. Growth* **132** 359 (1993)
89. I I Moiseev, M N Vargaftik, V V Volkov, G A Tsirkov, N V Cherkashina, V M Novotortsev, O G Ellert, I A Petrunenko, A L Chuvilin, A V Kvit *Mendeleev Commun.* 87 (1995)
90. A Henglein *Chem. Rev.* **89** 1861 (1989)
91. B G Ershov, E Janata, A Henglein *J. Phys. Chem.* **97** 339 (1993)
92. B G Ershov, E Janata, A Henglein, A Fojtik *J. Phys. Chem.* **97** 4589 (1993)
93. B G Ershov *Izv. Akad. Nauk, Ser. Khim.* 259 (1997) [e]
94. J Belloni *Curr. Opin. Colloid Interface Sci.* **1** 184 (1996)
95. A Henglein, D Meisel *Langmuir* **14** 7392 (1998)
96. A Henglein, M Giersig *J. Phys. Chem. B* **103** 9533 (1999)
97. A Takami, H Kurita, S Koda *J. Phys. Chem. B* **103** 1226 (1999)
98. B G Ershov *Izv. Akad. Nauk, Ser. Khim.* 1 (1999) [e]
99. K Esumi, A Suzuki, N Aihara, K Usui, K Torigoe *Langmuir* **14** 3157 (1998)
100. T Yonezava, N Toshima *J. Chem. Soc., Faraday Trans.* **91** 4111 (1995)
101. M Treguer, C de Cointet, H Remita, J Khatouri, M Mostafavi, J Amblard, J Belloni, R de Keyzer *J. Phys. Chem. B* **102** 4310 (1998)
102. M Michaelis, A Henglein, P Mulvaney *J. Phys. Chem.* **98** 6212 (1994)
103. N A Dhas, C P Raj, A Gedanken *Chem. Mater.* **10** 1446 (1998)
104. J S Bradley, E Hill, M E Leonowicz, H Witzke *J. Mol. Catal.* **41** 59 (1987)
105. S Kapoor *Langmuir* **14** 1021 (1998)
106. W Wang, X Chen, S Efrima *J. Phys. Chem. B.* **103** 7238 (1999)
107. C Roos, M Schmidt *Adv. Mater.* **11** 761 (1999)
108. S Chen, K Kimura *Langmuir* **15** 1075 (1999)
109. M Y Han, C H Quek, W Huang, C H Chew, L M Gan *Chem. Mater.* **11** 1144 (1999)
110. J N Golden, H Deng, F J DiSlavo, J M J Frecht, P M Tompson *Science* **268** 1463 (1995)
111. J J Watkins, T J McCarthy *Chem. Mater.* **7** 1991 (1995)
112. N Toshima, T Yonezawa, K Kushihashi *J. Chem. Soc., Faraday Trans.* **89** 2537 (1993)
113. K Meguro, Y Nakamura, Y Hayashi, M Torizuka, K Esumi *Bull. Chem. Soc. Jpn.* **61** 347 (1988)
114. T L Morkved, P Wiltzius, H M Jaeger, D G Grier, T A Witten *Appl. Phys. Lett.* **64** 422 (1994)
115. M Antonietti, A Thmnemann, E Wenz *Colloid Polym. Sci.* **274** 795 (1996)
116. L Bronstein, D Chernyshov, P Valetsky, N Tkachenko, H Lemmetyinen, J Hartman, S Förster *Langmuir* **15** 83 (1999)
117. C-W Chen, M Akashi *Langmuir* **13** 6465 (1997)
118. O E Litmanovich, A G Bogdanov, A A Litmanovich, I M Papisov *Vysokomol. Soedin., Ser. B* **39** 1875 (1997) [f]
119. O E Litmanovich, I M Papisov *Vysokomol. Soedin., Ser. A* **41** 1824 (1999) [f]
120. W Yu, H Liu *Chem. Mater.* **10** 1205 (1998)
121. V M Cepak, J C Hulteen, G Che, K B Jirage, B B Lakshmi, E R Fisher, C R Martin, H Yoneyama *Chem. Mater.* **9** 1065 (1997)
122. V M Cepak, C R Martin *J. Phys. Chem. B* **102** 9985 (1998)
123. M L Sandrock, C D Pibel, F M Geiger, C A Foss Jr *J. Phys. Chem. B* **103** 2668 (1999)
124. J V Zoval, J Lee, S Gorer, R M Penner *J. Phys. Chem. B* **102** 1166 (1998)
125. E S Shpiro, O P Tkachenko, N Jaeger, G Schulz-Ekloff, W Grünert *J. Phys. Chem. B* **102** 3798 (1998)
126. C W Hills, M S Nashner, A I Frenkel, J R Shapley, R G Nuzzo *Langmuir* **15** 690 (1999)
127. A Martino, S A Yamanaka, J S Kawola, D A Loy *Chem. Mater.* **9** 423 (1997)
128. J-H Gwak, S-J Kim, M Lee *J. Phys. Chem. B.* **102** 7699 (1998)
129. H Yanagi, S Mashiko, L A Nagahara, H Tokumoto *Chem. Mater.* **10** 1258 (1998)
130. G Ennas, A Mei, A Musinu, G Piccaluga, G Pinna, S Solinas *J. Non-Cryst. Solids* **232**–**234** 587 (1998)

131. M L Anderson, C A Morris, R M Stroud, C I Merzbacher, D R Rolison *Langmuir* **15** 674 (1999)
132. S Bharathi, N Fishelson, O Lev *Langmuir* **15** 1929 (1999)
133. S Efrima, B V Bronk *J. Phys. Chem. B* **102** 5947 (1998)
134. K Esumi, J Hara, N Aihara, K Usui, K Torigoe *J. Colloid Interface Sci.* **208** 578 (1998)
135. G S Attard, P N Bartlett, N R B Coleman, J M Elliott, J R Owen *Langmuir* **14** 7340 (1998)
136. Y Zhou, S H Yu, X P Cui, C Y Wang, Z Y Chen *Chem. Mater.* **11** 545 (1999)
137. P Hoenberg, W Kohn *Phys. Rev. B, Condens. Matter* **136** 864 (1964)
138. W Kohn, L J Sham *Phys. Rev. A.* **140** 1133 (1965)
139. P Ziesche, G Lehmann (Eds) *Ergebnisse in der Elektronen Theorie der Metalle* (Berlin: Academie-Verlag, 1983)
140. H English , R English *Phys. Status Solid* **124** 373 (1983)
141. E H Lieb *Phys. Rev. Lett.* **46** 457 (1981)
142. J P Pedrew, R G Parr, M Levy, J L Balduz *Phys. Rev. Lett.* **49** 1691 (1981)
143. R O Jones, O Gunnarsson *Rev. Mod. Phys.* **61** 689 (1989)
144. C O Almbladh, U von Barth *Phys. Rev. B, Condens. Matter* **31** 3231 (1985)
145. J P Perdew, W Yue *Phys. Rev. B, Condens. Matter* **33** 8800 (1986)
146. J P Perdew *Phys. Rev. B, Condens. Matter* **33** 8822 (1986)
147. A D Becke *Phys. Rev. A* **38** 3098 (1988)
148. C Lee, W Yang, R G Parr *Phys. Rev. B, Condens. Matter* **37** 785 (1988)
149. J P Perdew, J A Chevary, S H Vosko, K A Jackson, M R Pederson, D J Singh, C Fiolhais *Phys. Rev. B, Condens. Matter* **46** 6671 (1992)
150. O V Gritsenko, E J Baerends *Phys. Rev. A* **54** 1957 (1996)
151. P Süle, O V Gritsenko, A Nagy, E J Baerends *J. Chem. Phys.* **103** 10085 (1995)
152. A D Becke *J. Chem. Phys.* **104** 1040 (1996)
153. V I Roldughin, G A Martynov *Poverkhnost* (2) 19 (1988)
154. M Durand, P Schuck, X Vinas *Phys. Rev. A* **36** 1824 (1987)
155. K Takatsuka *Phys. Rev. Lett.* **61** 503 (1988)
156. M Casas, H Krivine, J Marorell *Eur. J. Phys.* **12** 105 (1991)
157. J Martorell, E Moya de Guerra *Ann. Phys.* **158** 1 (1984)
158. L D Landau, E M Lifshits *Kvantovaya Mekhanika* (Quantum Mechanics) (Moscow: Nauka, 1977)
159. E P Wigner *Phys. Rev.* **40** 749 (1932)
160. V P Silin *Vvedenie v Kineticheskuyu Teoriyu Gazov* (Introduction in the Kinetic Theory of Gases) (Moscow: Nauka, 1971)
161. B V Derjaguin, V I Roldughin *Surf. Sci.* **159** 69 (1985)
162. L K Grigor'eva, N S Lidorenko, E L Nagaev, S P Chizhik *Zh. Eksp. Teor. Fiz.* **91** 1050 (1986)
163. E M Lifshits, L P Pitaevskii *Statisticheskaya Fizika* (Statistical Physics) (Moscow: Nauka, 1978) Pt. 2
164. R Balian, C Bloch *Ann. Phys.* **60** 401 (1970)
165. R Kubo *J. Phys. Soc. Jpn.* **17** 975 (1962)
166. L P Gor'kov, G M Eliashberg *Zh. Eksp. Teor. Fiz.* **48** 1407 (1965)
167. E P Wigner *Ann. Math.* **53** 36 (1951)
168. E P Wigner *Ann. Math.* **62** 548 (1955)
169. F J Dyson *J. Math. Phys.* **3** 140 (1962)
170. M L Mehta, F J Dyson *J. Math. Phys.* **4** 713 (1963)
171. K B Efetov *Zh. Eksp. Teor. Fiz.* **83** 833 (1982)
172. M L Mehta *Random Matrices* (Boston: Academic Press, 1991)
173. R Denton, B Mühlschlegel, D J Scalapino *Phys. Rev.* **7** 3589 (1973)
174. E J Baerends, O V Gritsenko *J. Phys. Chem. A* **101** 5383 (1997)
175. W A de Heer *Rev. Mod. Phys.* **65** 611 (1993)
176. M Brack *Rev. Mod. Phys.* **65** 677 (1993)
177. W Ekardt, Z Penzar *Phys. Rev. B, Condens. Matter* **38** 4273 (1988)
178. W Ekardt, Z Penzar *Phys. Rev. B, Condens. Matter* **43** 1322 (1991)
179. E L Nagaev *Pis'ma Zh. Eksp. Teor. Fiz.* **48** 441 (1988)
180. V K Ivanov, A N Ipatov, V A Kharchenko *Zh. Eksp. Teor. Fiz.* **109** 902 (1996)
181. V K Ivanov, V A Kharchenko, M A Zhizhin *Pis'ma Zh. Eksp. Teor. Fiz.* **60** 345 (1994)
182. D M Wood, D Stroud *Phys. Rev. B, Condens. Matter* **28** 4374 (1983)
183. M P A Fisher, M Wortis *Phys. Rev. B, Condens. Matter* **29** 6252 (1984)
184. I T Iakubov, A G Khrapak, V V Pogosov, S A Trigger *Solid State Commun.* **56** 709 (1985)
185. I T Iakubov, A G Khrapak, V V Pogosov, S A Trigger *Solid State Commun.* **60** 377 (1986)
186. L I Kurkina, O V Farberovich *Fiz. Tv. Tela* **38** 1416 (1996)
187. L D Landau, E M Lifshits *Statisticheskaya Fizika* (Statistical Physics) (Moscow: Nauka, 1976) Pt. 1
188. Y Volokitin, J Sinzig, L J de Jongh, G Schmid, M N Vargaftik, I I Moiseev *Nature* (*London*) **384** 621 (1996)
189. Y E Volokitin, in Dr. Thesis, Leiden, 1997
190. B V Deryagin, N V Churaev, V M Muller *Poverkhnostnye Sily* (Surface Forces) (Moscow: Nauka, 1985)
191. V I Roldughin, B V Deryagin *Dokl. Akad. Nauk SSSR* **270** 642 (1983) [d]
192. V I Roldughin *Poverkhnost* (2) 126 (1985)
193. V I Roldughin, B V Deryagin *Kolloid. Zh.* **47** 322 (1985) [a]
194. B V Deryagin, L F Leonov, V N Yashin *Dokl. Akad. Nauk SSSR* **273** 122 (1983) [d]
195. B V Derjaguin, L F Leonov, V I Roldughin *J. Colloid Interface Sci.* **108** 207 (1985)
196. U Kreibig, M Vollmer *Optical Properties of Metal Clusters* (Berlin: Springer, 1995)
197. U Kreibig, in *Handbook of Optical Properties. Optics of Small Particles Interfaces and Surfaces* Vol. 2 (Eds R Hummel, P Wißmann) (Boca Raton, FL: CRC Press, 1997) p. 145
198. D C Ralph, C T Black, M Tinkham *Phys. Rev. Lett.* **74** 3241 (1995)
199. C T Black, D C Ralph, M Tinkham *Phys. Rev. Lett.* **76** 688 (1996)
200. M A Alvarez, J T Khoury, T G Schaaff, M N Shafigullin, I Vezmar, R L Whetten *J. Phys. Chem. B* **101** 3706 (1997)
201. U Kreibig, A Hilger, H Hövel, M Quinten, in *Large Clusters of Atoms and Molecules* (Ed. T P Martin) (Dordrecht: Kluwer Academic, 1996) p. 477
202. B M Sergeev, V A Kasaikin, E A Litmanovich, G B Sergeev *Kolloid. Zh.* **61** 712 (1999) [a]
203. J Rothe, J Hormes, H Bönnemann, W Brijoux, K Siepen *J. Am. Chem. Soc.* **120** 6019 (1998)
204. H Hövel, S Fritz, A Hilger, U Kreibig, M Vollmer *Phys. Rev. B, Condens. Matter* **48** 18 178 (1993)
205. K-P Charle, F Frank, W Shulze *Ber. Bunsenges. Phys. Chem.* **88** 350 (1984)
206. K A Sal'sedo, V V Tsvetkov, V D Yagodovskii *Zh. Fiz. Khim.* **64** 1858 (1990) [c]
207. A V Toporko, V V Tsvetkov, V D Yagodovskii, A Issa *Zh. Fiz. Khim.* **69** 867 (1995) [c]
208. A V Toporko, V V Tsvetkov, V D Yagodovskii, A Issa *Zh. Fiz. Khim.* **71** 1095 (1997) [c]
209. S K Donkpegan, V V Tsvetkov, N Yu Isaeva, V D Yagodovskii *Zh. Fiz. Khim.* **73** 1298 (1999) [c]
210. U Kreibig, M Gartz, A Hilger *Ber. Bunsenges. Phys. Chem.* **101** 1593 (1997)
211. A Kawabata, R Kubo *J. Phys. Soc. Jpn.* **21** 1765 (1966)
212. R Ruppin, H Yatom *Phys. Status Solidi B* **74** 647 (1976)
213. D M Wood, N W Ashcroft *Phys. Rev. B, Condens. Matter* **25** 6255 (1982)
214. A G Lesskin, V E Pasternak, A A Yushkanov *Zh. Eksp. Teor. Fiz.* **83** 310 (1982)
215. P M Tomchuk, B P Tomchuk *Zh. Eksp. Teor. Fiz.* **112** 661 (1997)
216. T Götz, W Hoheisel, M Vollmer, F Triger *Z. Phys. D* **33** 133 (1995)
217. A M Bonch-Bruevich, T A Vartanyan, Yu N Maksimov, S G Przhibel'skii, V V Khromov *Surf. Sci.* **307/309** 350 (1994);
218. W Hoheisel, M Vollmer, F Träger *Phys. Rev. B, Condens. Matter* **48** 17463 (1993)
219. R Monreal, S P Apell *Phys. Rev. B, Condens. Matter.* **41** 7852 (1990)
220. F Stietz , M Stucke, J Viereck, T Wenzel, F Träger *Surf. Sci.* **389** L1153 (1997)
221. T Götz, M Bergt, W Hoheisel, F Träger, M Stucke *Appl. Phys. A* **64** 149 (1997)
222. H Bönnemann, G Braun, W Brijoux, R Brinkmann, A Schulze Tilling, K Seevogel, K Siepen *J. Organomet. Chem.* **520** 143 (1996)
223. K Esumi, M Wakabayashi, K Torigoe *Colloids Surf. A* **109** 55 (1996)
224. M T Reets, W Helbig, A Quaiser *Chem. Mater.* **7** 2227 (1995)
225. H Bönnemann, W Brijoux, in *Advanced Catalysts and Nanosructured Materials* (Ed. W R Moser) (New York: Academic Press, 1996) p. 165

226. A Henglein *J. Phys. Chem.* **97** 5457 (1993)
227. P Mulvaney *Langmuir* **12** 788 (1996)
228. J A Creighton, D G Eadon *J. Chem. Soc., Faraday Trans.* **87** 3881 (1991)
229. A Henglein, Ch Brancewicz *Chem. Mater.* **9** 2164 (1997)
230. P Galletto, P F Brevet, H H Girault, R Antoine, M Broyer *J. Phys. Chem. B* **103** 8706 (1999)
231. F W Vance, B I Lemon, J T Hupp *J. Phys. Chem. B* **102** 10091 (1998)
232. Y-P Sun, J E Riggs, H W Rollins, R Guduru *J. Phys. Chem. B* **103** 77 (1999)
233. C D Keating, K K Kovaleski, M J Natan *J. Phys. Chem. B* **102** 9414 (1998)
234. M Quinten, D Schönauer, U Kreibig *Z. Phys. D* **12** 512 (1989)
235. U Kreibig *Z. Phys. D* **3** 239 (1986)
236. H M Lindsay, M J Lin, D A Weitz, P Sheng, Z Chen *Faraday Disc. Chem. Soc.* **83** 153 (1991)
237. V V Vysotskii, V I Roldughin *Kolloid. Zh.* **60** 729 (1998) [a]
238. V V Vysotsky, V I Roldughin *Colloid Surf.* **160** 171 (1999)
239. V M Shalaev, M I Shtokman *Zh. Eksp. Teor. Fiz.* **92** 509 (1987)
240. V A Markel', L S Muratov, M I Shtokman *Zh. Eksp. Teor. Fiz.* **98** 819 (1990)
241. H Hasegawa, N Satoh, K Tsujii, K Kimura *Z. Phys. D* **20** 325 (1991)
242. H Eckstein, U Kreibig *Z. Phys. D* **26** 2391993
243. K Kimura *J. Phys. Chem.* **98** 11997 (1994)
244. V V Slabko, S V Karpov, V I Zaitsev, A K Popov, G B Shevnina *J. Phys. Condens. Matter* **5** 7231 (1993)
245. S V Karpov, A K Popov, V V Slabko, G B Shevnina *Kolloid. Zh.* **57** 199 (1995) [a]
246. S V Karpov, A L Bas'ko, S V Koshelev, A K Popov, V V Slabko *Kolloid. Zh.* **59** 765 (1997) [a]
247. S V Karpov, A K Popov, V V Slabko *Izv. Akad. Nauk, Ser. Fiz.* **60** No6 43 (1996)
248. K Torigoe, K Esumi *Langmuir* **8** 59 (1992)
249. A Henglein *Ber. Bunsenges. Phys. Chem.* **99** 903 (1995)
250. A Henglein *Ber. Bunsenges. Phys. Chem.* **101** 1562 (1997)
251. S Wang, H Xin *J. Phys. Chem. B* **104** 5681 (2000)
252. V Vijayakrishnan, A Chainani, D D Sarma, C N R Rao *J. Phys. Chem.* **96** 8679 (1992)
253. D V Leff, L Brandt, J R Heath *Langmuir* **12** 4723 (1996)
254. L Genzel, T P Martin, U Kreibig *Z. Phys. B* **21** 339 (1975)
255. W P Halperin *Rev. Mod. Phys.* **58** 533 (1986)
256. A Hengleine *Israel J. Chem.* **33** 77 (1993)
257. E J Heilweil, R M Hochstrasser *J. Chem. Phys.* **82** 4762 (1985)
258. T W Roberti, B A Smith, J Z Zhang *J. Chem. Phys.* **102** 3860 (1995)
259. A E Faulhaber, B A Smith, J K Andersen, J Z Zhang *Mol. Cryst. Liq. Cryst.* **283** 25 (1996)
260. J Z Zhang, B A Smith, A E Faulhaber, J K Andersen, T J Rosales *Ultrafast Proces. Spectrosc.* **9** 561 (1996)
261. R H M Groeneveld, R Sprik, A Lagendijk *Phys. Rev. Lett.* **64** 784 (1990)
262. S D Brorson, J G Fujimoto, E P Ippen *Phys. Rev. Lett.* **59** 1962 (1987)
263. E D Belotskii, P M Tomchuk *Int. J. Electronics* **73** 955 (1992)
264. S A Gorban', S A Nepijko, P M Tomchuk *Int. J. Electronics* **70** 485 (1991)
265. T S Ahmadi, S L Logunov, M A El-Sayed *J. Phys. Chem. B* **100** 8053 (1996)
266. M Perner, P Bost, T Pauck, G von Plessen, J Feldmann, U Becker, M Menning, J Postendorfer, M Schmitt, H Schmidt *Springer Ser. Chem. Phys.* **62** 473 (1996)
267. M J Feldstein, C D Keating, Y-H Liau, M J Natan, N F Scherer *J. Am. Chem. Soc.* **119** 6638 (1997)
268. J H Hodak, I Martini, G V Hartland *Chem. Phys. Lett.* **284** 135 (1998)
269. P V Kamat, M Flumiani, G V Hartland *J. Phys. Chem. B* **102** 3123 (1998)
270. J H Hodak, I Martini , G V Hartland *J. Phys. Chem. B* **102** 6958 (1998)
271. A Stella , M Nisoli, S De Silvestri, O Svelto, G Lanzani, P Cheyssac, R Kofman *Phys. Rev. B, Condens. Matter* **53** 15497 (1996)
272. K Fauth, H Kreibig, G Schmid *Z. Phys. D* **20** 297 (1991)
273. B A Smith, J Z Zhang, U Giebel, G Schmid *Chem. Phys. Lett.* **270** 139 (1997)
274. R E Benfield , J A Creighton, D G Eadon, G Schmid *Z. Phys. D* **12** 533 (1989)
275. J H Hodak, I Martini , G V Hartland *J. Chem. Phys.* **108** 9210 (1998)
276. A Tamura, K Higeta, T Ichinokawa *J. Phys. C, Solid State Phys.* **15** 4975 (1982)
277. H Fujiwara, S Yanagida, P V Kamat *J. Phys. Chem. B* **103** 2589 (1999)
278. H R Zeller, I Giaver *Phys. Rev.* **181** 789 (1969)
279. L S Kuz'min, K K Likharev *Pis'ma Zh. Eksp. Teor. Fiz.* **45** 389 (1987)
280. J B Barner, S T Ruggiero *Phys. Rev. Lett.* **59** 109 (1987)
281. P J M van Bentum, R T M Smokers, H van Kempen *Phys. Rev. Lett.* **60** 2543 (1988)
282. R Wilkins, E Ben-Jacob, R C Jaclevic *Phys. Rev. Lett.* **63** 801 (1989)
283. R S Ingram, M J Hostetler, R W Murray, T G Schaaff, J T Khoury, R L Whetten, T P Begioni, D K Guthrie, P N First *J. Am. Chem. Soc.* **119** 9279 (1997)
284. T Sato, H Ahmed *Appl. Phys. Lett.* **70** 2759 (1997)
285. D L Klein, P L McEuen, J E B Katari, R Roth, A P Alivisatos *Appl. Phys. Lett.* **68** 2574 (1996)
286. L C Brousseau , Q Zhao, D A Shultz, D L Feldheim *J. Am. Chem. Soc.* **120** 7645 (1998)
287. S Chen, R W Murray, S W Feldberg *J. Phys. Chem. B* **102** 9898 (1998)
288. S-T Yau, P Mulvaney, W Xu, G M Spinks *Phys. Rev. B, Condens. Matter* **57** R15124 (1998)
289. S P Gubin, E S Soldatov, A S Trifonov, V V Khanin *Mendeleev Commun.* 30 (1997)
290. L I Glazman, K A Matveev *Zh. Eksp. Teor. Fiz.* **98** 1834 (1990)
291. C Weisbuch, B Binter *Quantum Semiconductor Structures* (New York: Academic Press, 1991)
292. A P Alivisatos *Science* **271** 933 (1996)
293. L Banyai, S W Koch *Semiconductor Quantum Dots* (Singapore: Word Scientific, 1993)
294. H Brune *Surf. Sci. Rep.* **31** 121 (1998)
295. G Fucks, P Melinon, F D Santos Aires, M Treilleux, B Cabaud, A Hoareau *Phys. Rev. B, Condens. Matter* **44** 3926 (1991)
296. H Haberland, Z Insepov, M Moseler *Phys. Rev. B, Condens. Matter* **51** 11061 (1995)
297. A Perez, P Melinon, V Dupuis, P Jensen, B Prevel, J Tuaillon, L Bardotti, C Martet, M Treilleux, M Broyer, M Pellarin, J L Vaille, B Palpant, J Lerme *J. Phys. D, Appl. Phys.* **30** 709 (1997)
298. P Jensen *Rev. Mod. Phys.* **71** 1695 (1999)
299. J A Dagata, J Schneir, H H Harary, C J Evans, M T Postek, J Bennet *Appl. Phys. Lett.* **56** 201 (1990)
300. H Sugimura, T Uchida, N Kitamura, H Masuhara *J. Phys. Chem.* **98** 4352 (1994)
301. N Kramer, H Brik, J Jorristma, C Schönenberger *Appl. Phys. Lett.* **66** 1325 (1995)
302. E S Snow, P M Campbell *Science* **270** 1639 (1995)
303. J C Hulteen, D A Treichel, M T Smith, M L Duval, T R Jensen, R P van Duyne *J. Phys. Chem.* **103** 3854 (1999)
304. J K Schoer, R M Crooks *Langmuir* **13** 2323 (1997)
305. S-W Tam-Chang, H A Biebuyck, G H Whiteside, N Jeon, R J Nuzzo *Langmuir* **11** 4371 (1995)
306. E Delamarche, A C F Hool, B Michel, S Wilkes, M Despont, M E Welland, H Biebuyck *J. Phys. Chem. B* **101** 9263 (1997)
307. J Boneberg, F Burmeister, C Schifle, P Leiderer, D Reim, A Fery, S Herminghaus *Langmuir* **13** 7080 (1997)
308. C B Murray, C R Kagan, M G Bawendi *Science* **270** 1335 (1995)
309. H Weller *Angew. Chem., Int. Ed. Engl.* **35** 1079 (1996)
310. D Bethell, M Brust, D J Schiffrin, C J Kiely *J. Electroanal. Chem.* **409** 137 (1996)
311. R P Andres, J D Bielefeld, J I Henderson, D B Janes, V R Kolaguta, C P Kubiak, W J Mahoney, R G Osifchin *Science* **273** 1690 (1996)
312. Z L Wang, S A Harfenist, I Vezmar, R L Whetten, J Benthley, N D Evans, K B Alexander *Adv. Mater.* **10** 808 (1998)

313. P C Ohara, D V Leff, J R Heath, W M Gelbart *Phys. Rev. Lett.* **75** 3466 (1995)
314. A Badia, L Cuccia, L Demers, F Morin, R B Lennox *J. Am. Chem. Soc.* **119** 2682 (1997)
315. S Murthy, Z L Wang, R L Whetten *Philos. Mag. Lett.* **75** 321 (1997)
316. M D Musick, C D Keating, M H Keefe, M J Natan *Chem. Mater.* **9** 1499 (1997)
317. P C Ohara, J R Heath, W M Gelbart *Angew. Chem., Int. Ed. Engl.* **36** 1078 (1997)
318. M Brust, D Bethell, D J Schiffrin, C J Kelly *Adv. Mater.* **7** 795 (1995)
319. J Fink, C J Kiely, D Bethell, D J Schiffrin *Chem. Mater.* **10** 922 (1998)
320. Z L Wang *Adv. Mater.* **10** 13 (1998)
321. Z L Wang, S A Harfenist, R L Whetten, J Bentley, N D Evans *J. Chem. Phys. B* **102** 3068 (1998)
322. W D Luedtke, U Landman *J. Phys. Chem.* **100** 13323 (1996)
323. B A Korgel, S Fullam, S Connolly, D Fitzmaurice *J. Phys. Chem. B* **102** 8379 (1998)
324. W M Gelbart, R P Sear, J R Heath, S Chaney *Faraday Discuss.* **112** 299 (1999)
325. X M Lin, C M Sorensen, K J Klabunde *Chem. Mater.* **11** 198 (1999)
326. A Taleb, C Petit, M P Pileni *J. Chem. Phys. B* **102** 2214 (1998)
327. J J Shiang, J R Heath, C P Collier, R J Saykally *J. Phys. Chem. B* **102** 3425 (1998)
328. A H Lu, G H Lu, A M Kessinger, C A Foss Jr *J. Phys. Chem. B* **101** 9139 (1997)
329. L-Z Wang, J-L Shi, W-H Zhang, M-L Ruan, J Yu, D-S Yan *Chem. Mater.* **11** 3015 (1999)
330. K Bandyopodhyay, V Patil, K Vijayamohanan, M Sastry *Langmuir* **13** 5244 (1997)
331. S N Rao, D Fitzmaurice *Helv. Chim. Acta* **81** 902 (1998)
332. L Cusack, R Rizza, A Gorelov, D Fitzmaurice *Angew. Chem., Int. Ed. Engl.* **36** 848 (1997)
333. F C Meldrum, N Kotov, J H Fendler *Chem. Mater.* **7** 1112 (1995)
334. M Giersig, P Mulvaney *J. Phys. Chem.* **97** 6334 (1993)
335. M Trau, D A Saville, I A Aksay *Langmuir* **13** 6375 (1997)
336. J P Spatz, A Rouscher, M Moller *Adv. Mater.* **8** 337 (1996)
337. R W Zehner, W A Lopes, T L Morkved, H M Jaeger, L R Sita *Langmuir* **14** 241 (1998)
338. V M Rudoi, I V Yaminskii, O V Dement'eva, V A Ogarev *Kolloid. Zh.* **61** 861 (1999) [a]
339. S L Burkett, S Mann *Chem. Commun.* 321 (1996)
340. A P Alivisatos, K P Johnsson, X Peng, T E Wilson, C J Loweth, M P Bruchez Jr, P G Schultz *Nature* (*London*) **382** 609 (1996)
341. C A Mirkin, R L Letsinger, R C Mucic, J J Storhoff *Nature* (*London*) **382** 607 (1996)
342. R C Mucic, J J Storhoff, C A Mirkin, R L Letsinger *J. Am. Chem. Soc.* **120** 12674 (1998)
343. S Connolly, D Fitzmaurice *Adv. Mater.* **11** 1202 (1999)

[a] — *Russ. Colloid J. (Engl. Transl.)*
[b] — *High Energy Chem. (Engl. Transl.)*
[c] — *Russ. J. Phys. Chem. (Engl. Transl.)*
[d] — *Dokl. Chem. Technol., Dokl. Chem. (Engl. Transl.)*
[e] — *Russ. Chem. Bull. (Engl. Transl.)*
[f] — *Polym. Sci. (Engl. Transl.)*